13

Channel Replacement Therapy for Cystic Fibrosis

John M. Tomich, Urška Bukovnik, Jammie Layman and Bruce D. Schultz
Departments of Biochemistry and Anatomy and Physiology
Kansas State University, Manhattan, Kansas
USA

1. Introduction

Epithelial monolayers act as barriers to the movement of small solute molecules – including both inorganic ions and drugs – between body compartments. Ions traverse epithelial apical and basolateral membranes *via* a combination of tightly regulated ion-specific transporters and channels. Compromised function of any component leads to electrolyte and fluid imbalances resulting in morbidity and potentially, mortality. In the case of cystic fibrosis (CF) the defect lies in various genotypes that result in suboptimal synthesis, folding, transport, or gating of the CF transmembrane conductance regulator (CFTR; an anion channel that has other reported cellular functions). Many of the current therapies involve palliative interventions that address infections, inflammation, nutrition and mucus viscosity issues in patients. While these approaches have increased the life span of CF patients by reducing the rate of decline in lung functions or other health issues, none of them addresses the underlying cause of the disease at the cellular or tissue level, namely reduced anion conductance that sets the chemiosmotic driving force for both paracellular and transcellular fluid movement.

Many recent studies focus on small molecule approaches to rescue some forms of CFTR that are defective with respect to folding, intracellular trafficking, or activity. Of particular note has been the identification of VX-770, a small molecule that restores CFTR activity in patients harboring the G551D mutation. Results of a phase 3 clinical trial showed that VX-770 improved lung function by 10.5 percent over the placebo and achieved all secondary goals of the study (Accuroso et al., 2010). This is the first drug to show improvement in lung function in patients with the G551D mutation. Unfortunately, such profound effects of this drug have not been realized when tests were conducted with patients harboring other CFTR mutations. Other small molecules that may affect other forms of CFTR (e.g., ataluren for premature stop codons) are in the pipeline, although none appears to be as advanced as VX-770.

The idea of using small pore-forming peptides to treat various channelopathies has been an ongoing objective since identifying the pore-defining M2 transmembrane (TM) segment in the α-subunit of the spinal cord glycine receptor (GlyR) Cl^- channel in the early 1990's (Reddy et al., 1993). The parent sequence, M2GlyR, is the pore-forming segment of the Cl^-

selective human spinal cord glycine receptor. In Wallace et al., (1992), we first suggested that inserting exogenous Cl^- channel-forming peptides into the apical membranes of airway epithelial cells of CF patients may aid in restoring the ability of these cells to secrete fluid. This was the rationale for developing synthetic Cl-conducting channel-forming peptides as potential therapeutic agents. We have since developed synthetic peptides that form pores with varying degrees of anion conduction and selectivity. A guiding goal has been the *de novo* generation of a pore that could be used as a general therapeutic for CF since it would not require genotyping of individual patients. This novel therapeutic intervention, which would provide a new conductance pathway for selected anions, lies midway between conventional drug therapy and gene therapy. The primary target tissue, airway epithelium is accessible to aerosolized formulations such that the therapeutic peptides could be delivered easily.

The ideal therapeutic channel-forming peptide should: 1) have high aqueous solubility as a monomer; 2) have no detectable antigenicity; 3) bind to and then partition into biological membranes rapidly at low solution concentrations; 4) undergo supramolecular assembly in the membrane to form pores with measurable ion throughput; and 5) show physiologically relevant anion selectivity. All of these targeted outcomes have been achieved with the exception of the final goal, anion selectivity. In this regard, we are exploring distinct approaches to raise the permselectivity for Cl^- (P_{Cl}) relative to both Na^+ and K^+.

Cells exposed to our *de novo* peptides that form membrane pores appear to tolerate them well, with net anion flux controlled by the natural regulation of counter-ion transport and/or anion loading. Using a combination of peptide synthesis, electrophysiology, structural biology and computer simulations we are endeavoring to prepare highly anion-selective channels. Numerous studies have been performed that switch anion to cation selectivity and vice-versa (see review-Keramidasa et al., 2004). Our studies targeting enhanced anion selectivity are novel and will yield a lead compound for treating CF as well as aid in our understanding of anion selectivity in channel proteins. The work is being accomplished by preparing sequences with rational alterations to the residues that dictate the chemical composition and structure of the pore.

This chapter will review our extensive exploration of the permissible amino acid replacements in the M2GlyR sequence based on knowledge of Cl^- binding motifs and channel architecture. Modifications to the channel forming peptides were based on a wealth of data obtained from the fields of inorganic chemistry, channel physiology, structural determinations and computer modeling. The channel-forming peptides discovered during this project are remarkable in several ways: 1) they are small and easily synthesized; 2) they are water soluble and can be delivered to membrane surfaces without added organic solvents; 3) most are predominantly monomeric in solution; 4) when inserted into membranes, all peptides are expected to be oriented in the same direction due to the highly positively charged N-terminus; 5) all assembled pores are composed with a parallel orientation of the helices; 6) functional ion conducting pores are formed that can provide information on various channel properties; and 7) the small size of the peptides and the assembled pores facilitate concerted efforts for structural analyses and computer modeling that can produce informative structures.

To our knowledge no other membrane/peptide system offers such flexibility for design and analysis. Many TM sequences have been and are being studied by others (Marsh, 1996). However, for the most part, incorporation into bilayers leads to a mixed orientation with helical dipoles present in both directions. Such mixing of dipole orientations is prevented in our oligo-lysine adducted M2GlyR peptide system. This review will describe our understanding of how these peptides form channels with a range of anion selectivity and conductance properties, through a combination of electrophysiology, biophysical structural studies and computer simulations.

2. Current CF therapies

While a number of therapies for CF are currently in development, many of the treatment options presently available to patients are palliative in nature, addressing one or more symptoms of the condition and acting to reduce the severity of these effects and their associated risks.

Diet/nutritional supplements Proper diet and nutrition may reduce the impact and risk of CF-related conditions such as diabetes and osteoporosis. The lungs of CF patients appear to have fewer natural antioxidants than those without the condition, which may contribute to repeated infection and persistent inflammation. Patients may benefit from an increase in their intake of antioxidants through diet or supplements to fight this inflammation. Further promise may lie in drugs that work to build antioxidants in the lungs. AquADEKs® by Yasoo Health, Inc. is a vitamin supplement specifically formulated to meet the antioxidant needs of those with CF, and is commercially available. It has been shown to improve lung function, normalize vitamin levels in plasma and reduce neutrophilic inflammation (Sagel et al., 2011).

Enzyme replacement therapies Pancreatic enzyme products work to increase the digestion and absorption of fats, proteins, and starches while promoting the absorption of certain vitamins in those with CF, who often suffer from malnutrition due to enzyme deficiencies. The U.S. Food and Drug Agency (FDA) has approved a number of these products, including Zennen® (Eurand Pharmaceuticals), Creon® (Abbott Laboratories) and Pancreaze™ (Ortho-McNeil Pharmaceutical), while others, such as Pancrecarb® (DCI) and Ultrase® (Axcan Scandipharm) are still awaiting clinical trials. Liprotamase® (Alnara Pharmaceuticals) is a non-porcine pancreolipase enzyme therapy, which has completed a phase 3 clinical trial. However, the new drug application submitted by Alnara was rejected by the FDA on the grounds of insufficient data demonstrating the efficacy of the drug (Lowry, 2011).

Antibiotics/anti-infectives Due to the increased risk of disease caused by the excess and/or viscous mucus that is characteristic of CF, patients are often treated with antibiotics to circumvent chronic infections, such as that of *Pseudomonas aeruginosa*. Antibiotics can be administered orally, intravenously, via inhalation through devices such as metered dose inhalers (MDIs), or through implanted devices such as a port or Peripherally Inserted Central Catheter (PICC) (Gibson et al. 2003). TOBI® (tobramycin solution for inhalation) and recently developed Cayston® (aztreonam solution for inhalation) are two approved and commonly prescribed antibiotics for patients with CF, and both are effective against *P. aeruginosa*. TOBI® is approved to treat P. aeruginosa infections by concentrating the delivery of the antibiotic to the airways. Developed by Novartis Pharmaceuticals and widely

used worldwide since its FDA approval in 1997, TOBI® has been successful in improving overall lung function while reducing hospital stays for CF patients (Cheer et al., 2003). TIP (TOBI® Inhalation Powder) is a new form of tobramycin that takes less time to administer via a Podhaler® and exhibits the same efficacy as the original formulation. It has been approved for use in Canada (http://www.pharmiweb.com/pressreleases/pressrel.asp?ROW_ID=23942 and http://www.novartis.com/newsroom /media-releases/en/2010/1446760.shtml). Cayston® (formerly GS9310/11) by Gilead Sciences is a newly developed version of the antibiotic aztreonam lysine in aerosol form. It was approved by the FDA and has been available to CF patients since February of 2010 (http://www.accessdata.fda.gov/scripts/cder/drugsatfda/ index.cfm?fuseaction=Search.DrugDetails).

The macrolide antibiotic azithromycin (Pfizer, Inc.) has been shown, when administered orally, to fight *P. aeruginosa* infection and improve pulmonary function in CF patients aged 6 years and older. Further studies are required to determine efficacy of prolonged treatment and in treating those under 6 years of age (Saiman et al., 2003). Further, azithromycin (Delete "the common antibiotic") was shown in phase 3 trials to preserve healthy lung function in CF patients (Saiman et al., 2010). Several other anti-infective agents, which are presently being evaluated, are discussed in brief below. Mpex Pharmaceuticals has recently developed MP-376, an aerosol form of levofloxacin, used to treat *P. aeruginosa* infections in the lungs. Phase 3 trials are currently underway (http://www.mpexpharma.com/mp-376.html). Insmed Incorporated recently completed phase 2 trials of Arikace™, a version of the FDA-approved antibiotic amikacin in a liposomal formulation that is inhaled using a nebulizer. It was shown in animal studies to decrease the pathogenicity of *P. aeruginosa* and has demonstrated success in permeating human sputum in the lungs. Phase 3 trials are set to begin in late 2011 (http://www.insmed.com/arikace.php). Bayer Schering Pharmaceuticals' BAY Q3939, was developed as a new inhaled version of the drug ciprofloxacin to more effectively treat infections in air passages. Phase 2 trials for the drug are currently underway (http://clinicaltrials.gov/ct2/show/NCT00645788).

Mucolytics/Airway-Rehydrating Agents Since viscous mucus build-up in the lungs can promote bacterial infections, many therapies are directed toward reducing the symptom by restoring the liquid necessary to hydrate the mucus or the underlying layer to facilitate expectoration (Pettit and Johnson, 2011) or, in the case of Pulmozyme® and other agents, to reduce mucus viscosity. Pulmozyme® by Genentech is a Dornase alfa (recombinant human deoxyribonuclease) treatment used to break down the DNA responsible for thickening pulmonary mucus and thus to reduce viscosity, promote mucus clearing, and ultimately restrict (delete "to", replace "reduce" with "restrict") the environment that supports bacterial growth. Approved in 1993 and introduced in 1994, Pulmozyme® is currently in use as a mucolytic for patients with CF and has been shown to increase lung function by about 6% and reduce the risk of infection by 27% (Fuchs et al., 1994; http://www.pulmozyme.com/hcp/prescribing-info.jsp#table1). Moli1901 by Lantibio stimulates alternative Cl^- channels in order to compensate for the deficiencies of CFTR in the pulmonary epithelium of patients. In phase 2 European trials, Moli1901 was well tolerated in most patients (one participant experienced a transient decrease in pulmonary function). Those receiving treatment of 2.5 mg daily of inhaled Moli1901 showed significant improvement in lung function measured as forced expiratory volume in one second (FEV_1; Grasemann et al., 2007).Initially promising, Denufosol, a P2Y2 agonist developed by Inspire,

was believed to rehydrate the airway surface liquid, bypassing the basic CFTR protein defect, producing improvement in pulmonary function (Kellerman et al., 2008). However, the most recent clinical trial found it to be without effect. GS9411 by Gilead is an epithelial Na^+ channel (ENaC) inhibitor, which blocks Na^+ absorption in airways to reduce mucus dehydration. A phase 1 trial of GS9411 has been completed and the drug was shown to be safe and well tolerated (Sears et al., 2011; http://clinicaltrials.gov/ct2/show/NCT00999531).

An Australian clinical trial showed that a mist of hypertonic saline delivered via nebulizer twice daily for one year helped to improve lung function and reduce lung infections. The study included participants 6 years of age and older with mild or moderate lung disease (however, those with *Burkholderia cepacia* were not included in the study). The study tested two groups, one receiving "normal saline" solution at 0.9%, and the other receiving the "hypertonic saline" solution at 7% salt. While both groups showed improvement in pulmonary function during the study, those receiving hypertonic saline exhibited significantly greater improvement than those on normal saline. Elkins et al. (2006) reported that hypertonic saline also caused a reduction in exacerbations from the lungs, and Donaldson et al. (2008) hypothesized that this was due to the "protection" by hypertonic saline of non-obstructed airways from further mucus build-up and bacterial infection.

Similarly, an inhaled version of mannitol was shown to help clear CF airways and improve pulmonary function by an average of 7.3% (FEV_1) and forced airway flow by 15.5%. Mannitol works by drawing water into the lungs osmotically and thus helping to clear mucus. No serious adverse side effects were observed and it appeared to be well tolerated by patients (Jaques et al., 2008; Bilton et al., 2011). Phase 3 trials have been completed and the therapy is currently being marketed in Europe, and Pharmaxis hopes to submit a new drug application for Bronchitol to the FDA (http://www.pharmaxis.com.au/assets/pdf/2010/15122010).

Anti-Inflammatories Due to the recruitment of macrophages and neutrophils during rounds of bacterial infection, collateral damage to host airway cells by nuclear factor (NF)-*kappa* B activation and elevated pro-inflammatory cytokines leads to scarring and fibrosis. A number of anti-inflammatory agents are currently being used or studied to determine their efficacy in reducing inflammation in the pulmonary passages of CF patients. The over-the-counter drug, ibuprofen, taken orally twice daily at dosages adjusted to give peak plasma concentrations of 50 to 100 micrograms per milliliter, reportedly reduced the decline of lung function (Konstan et al., 1995). Oral N-acetylcysteine (PharrmaNAC, BioAdvantex Pharma, Inc.) was shown in clinical trials to reduce inflammation and increase pulmonary function by restoring glutathione in neutrophils. A phase 2 trial has completed enrolling subjects recently (Tirouvanziam et al., 2006; Atkuri et al., 2007). In a similar approach, inhaled doses of glutathione have completed phase 2 trials in Germany and data will be available in late 2011 (Retsch-Bogart, 2007). A University of Massachusetts study was conducted to test the efficacy of adding the fatty acid docosahexaenoic acid (DHA) to fortify infant formula in reducing CF pathogenicity. This work is based on the observation that an imbalance in fatty acids can lead to inflammation. It is hypothesized that an increase in DHA can help reduce inflammation that occurs with CF-related imbalances. Results of the study will be available in 2011. Genzyme Corp., which has licensed the patent as a treatment for CF, is considering new and more effective means of delivering DHA (Freedman et al., 1999; 2004). KB001

produced by Kalobios Pharmaceuticals reduces local inflammation from the virulence factor of *P. aeruginosa*. *P. aeruginosa* uses the structure of its Type Three Secretion System (TTSS) to break through cellular membranes and release toxins. KB001 binds to the PcrV protein essential to TTSS and inhibits its activity, reducing pathogenicity and preserving the immune defense of the host against *P. aeruginosa*. Though KB001 may reduce pathogenicity of *P. aeruginosa*, thereby preventing inflammation, it does not appear to affect in vivo growth of the bacteria, and thus is not classified as an anti-infective (Baer et al., 2008; http://www.kalobios.com/kb_pipeline_001.php). A recent report showed that an inhaled phosphodiesterase type 5 inhibitor, sildenafil, increased Cl^- transport in mice (Lubamba et al., 2011). Further research at the University of Wales suggested that sildenafil may assist in intracellular trafficking of the ΔF508-CFTR gene protein (Dormer et al., 2005). The corticosteroid, GSK SB 656933 manufactured by GlaxoSmithKline is an inhaled dose of fluticasone propionate used to treat lung inflammation was shown to be safe and tolerated in CF patients in phase 1 clinical trials (Lazar et al., 2011; http://www.clinicaltrials.gov/ct2/show/NCT00903201?term=656933&rank=5NLM Identifier: NCT00903201). The drug is currently used to reduce pulmonary inflammation in chronic obstructive pulmonary disease (COPD).

Experimental CF Therapies Aside from gene therapy, some new experimental approaches are aimed at modifying the folding or translocation of the endogenous mutant CFTR proteins in order to generate a functional channel protein at the cell surface. Correcting these defects would re-establish transcellular flow of Cl^-, Na^+, and water to clinically relevant levels to provide appropriate airway surface liquid volume and composition (http://www.cff.org/treatments/Pipeline/).

CF Gene Therapy is directed toward correcting the channelopathy by incorporating DNA that encodes for the full-length wild-type CFTR protein. Research suggests that CFTR gene expression is required at a mere 5% of the normal level in order to improve pulmonary function (Ramalho et al., 2002). There are a number of gene therapy protocols currently under investigation with the frontrunners discussed below.

Compacted DNA (PLASmin®): (unbold. Inconsistent) One problem in developing a treatment for CF through gene therapy is that non-viral DNA must be condensed, which is commonly achieved through the use of polycations. However, this often results in a complex that is too large to cross the cellular membrane effectively and deliver DNA to the affected cells. Cleveland-based Copernicus Therapeutics, Inc. developed a compacted DNA/DNA nanoparticle therapy (PLASmin®) that decreases the volume of the complex by up to 1000-fold, to a single molecule small enough to permeate the membrane and nuclei of target cells. The complex contains only one copy of the DNA to be delivered, increasing the stability and efficacy of the treatment (Chen et al., 2007). In phase 1a trials, plasmid DNA nanoparticles with the gene responsible for encoding CFTR were applied intra-nasally with lysine peptides substituted with polyethylene glycol. About two-thirds of the participants in the study showed a significant improvement and results persisted for up to 6 days. No adverse side effects of considerable severity were observed as a result of the compacted DNA. However, this trial presented no demonstration of gene expression (Konstan et al., 2004). More recently, Copernicus has experienced greater success with the level and duration of CFTR expression in animal models

(http://www.thefreelibrary.com/Copernicus+
Receives+Milestone+Payment+from+Cystic+ Fibrosis+Foundation...-a0172302400).

VX-770 (Ivacaftor; Vertex Pharmaceuticals) is a novel therapy that seeks to augment CFTR activity in patients harboring the G551D mutation. This small molecule is a CFTR "potentiator" that increases function of faulty CFTR proteins by holding the defective channels in the open conformation. This treatment has completed phase 1 and phase 2 trials, which have shown efficacy in reducing sweat Cl^- concentrations and increasing nasal potential difference measures as well as improvements in general lung health. VX-770 replicated these results in two phase 3 trials – one for ages 12 and above (adult) and one for ages 6-11 (child). Both trials showed relevant increases in FEV_1 of 10.6% and 12.5% for each age group respectively over the placebo groups. VX-770 also helped patients in the trials gain weight – nearly 7 pounds on average for the adult trial and about 8 pounds for the children's trial. Finally, the phase 3 trials also showed increases in general lung health, indicated the treatment was well tolerated, and demonstrated lower sweat Cl^- levels. This closer to normal Cl^- range is very important to note as it provides empirical evidence that VX-770 is effectively treating the cause of CF and not just its symptoms. Vertex plans to submit a new drug application (NDA) to the FDA in late 2011 for VX-770 (Sheridan, 2011).

VX-809 in conjunction with VX-770: VX-809 is a novel small molecule CFTR "corrector" being developed by Vertex Pharmaceuticals that seeks to augment channel activity in CF patients with the ΔF508 CFTR mutation when used in conjunction with VX-770. The ΔF508 mutation affects 87% of CF patients in the United States (48% of patients have both mutant alleles while 39% have one). Misfolding of the mutated protein interferes with cytosolic trafficking such that the protein never reaches the apical membrane, precluding any anion secretion. VX-809 partially corrects the defect by promoting the trafficking of CFTR proteins to its proper location in the apical membrane. ΔF508 CFTR has a reduced open probability. Thus, VX-809 is paired with VX-770, the CFTR "potentiator", in the hopes of increasing total protein function for maximum effect on the disease. A phase 2 trial testing various dose combinations of the two compounds met its primary endpoints of safety and efficacy in the first part of the trial. Patients harboring the ΔF508 mutation were given VX-809 or a placebo for 14 days and then a combination VX-809 and VX-770 or a placebo for 7 more days. The drugs were well tolerated, though about half of patients did report some adverse respiratory events, none of which were deemed serious. Furthermore, the most effective combination regiment showed significant total reductions in the sweat Cl^- levels of 13 mmol/L from a baseline of ~100 mmol/L. The 14 days of solely VX-809 reduced sweat Cl^- by 4 mmol/L. This is strong evidence that, first, VX-809 is able to direct CFTR to its operational location and, second, that VX-770 is able to increase the function of this most common mutated form of CFTR once it has been moved to that location. The final part of this study will begin at the end of 2011 (Pollack, 2011; and http://investors.vrtx.com/releasedetail.cfm?releaseid= 583683).

Ataluren (formerly known as PTC124®) is a protein restoration therapy that helps produce working copies from mutated forms of CFTR that harbor nonsense mutations (nmCF). Pioneered by PTC Therapeutics, Ataluren® is a small molecule compound that has shown clinical promise through phase 2 trials in the alleviation of several genetic disorders caused by nonsense mutations, including nmCF. Exclusively targeting nonsense

mutations, ataluren® overrides the premature stop codons symptomatic of these mutations to allow for the completion of the desired protein. In the case of nmCF, a small (19 participant) phase 2 trial showed an ability to produce viable, working copies of CFTR via this "ribosomal read through" mechanism. The study showed significant improvements in total Cl^- channel activity, measured by nasal transepithelial potential difference, which increased over time and led to improved pulmonary function and coughing. Ataluren was able to do this without interfering with other properly functioning stop codons, allowing the CFTR protein to be translated as initially designed and making the compound safe to administer. All trials of the compound have shown it to be well tolerated in humans with side effects mild and sparse to date. Ataluren®is currently in a 48 week CF phase 3 trial seeking statistically significant increased lung function, measured by FEV_1 as its primary endpoint with safety and drug activity as secondary endpoints. Ataluren has orphan status from the FDA and European Commission as well as Subpart E for expedited development from the FDA. The phase 3 trial data will become available in the first half of 2012 (Wilschanski et al., 2011; and http://www.ptcbio.com/3.1.1_genetic_disorders.aspx).

3. Channel replacement therapy

As indicated above, there are numerous approaches to treating this channelopathy. Combinations of these treatment modalities have increased the lifespan of those afflicted from 4, to now greater than 35 years of age. Perhaps the most significant of these therapies has been the use of pancreatic enzyme replacements, anti-inflammatories and powerful antibiotics. While restoration of CFTR activity has been an ultimate goal through CFTR rescue and in particular gene therapy, these therapeutic approaches have helped only limited numbers of patients. We have advocated another approach: *peptide-based channel replacement therapy*. Under this scenario a channel-forming peptide is applied to the apical surface of CF airway tissues to promote anion secretion and surface hydration. Gene therapy, to date, has involved the delivery of a CFTR-encoding DNA segment encased in a viral capsid to the affected epithelial tissues. There are serious problems with the gene therapy delivery vectors, transformation efficiency and CFTR production and delivery. Also airway epithelial cells have limited half-lives and the airway would need to undergo gene therapy on a regular basis to maintain expression. The new approach described here is much simpler (administered at home) and places the therapeutic directly on the target membrane (**Fig. 1**). Our efforts have been focused on developing a membrane-active peptide that can be delivered efficiently, assemble into a Cl^- selective pore, trigger fluid secretion and elicit no detectable immune or inflammatory responses. The remainder of this chapter traces the development of this treatment modality. While many of the desired properties have been incorporated into this therapy some hurdles remain. These will be discussed later in the chapter.

Chloride Channels Ion channels are usually multi-subunit protein molecules that have gated water-lined pores and an ion selectivity filter. Channels are individually gated by a variety of signals including ligands, non-covalent and covalent modifications, voltage, and/or mechanical stimuli. In most biological fluids, the most relevant physiological cations and anions are Na^+, K^+, and Ca^{2+}; and Cl^-, and HCO_3^-, respectively. An extensive literature is available to clearly document the high selectivity of naturally occurring cation channels in both excitable and non-excitable tissues (e.g., K_v, Na_v, ENaC, Ca_v, etc.). Three major classes of Cl^- channels have been cloned and studied. These include 1) the ligand gated channels

typified by inhibitory post-synaptic glycine, glutamate and GABA receptors; 2) CFTR, which is an ABC transporter family member exhibiting complex nucleotide-dependent gating; and 3) ClC channels, which appear to be ubiquitous and are both voltage and metabolically gated. Ion channel classes display significant structural differences in the conductive pathway.

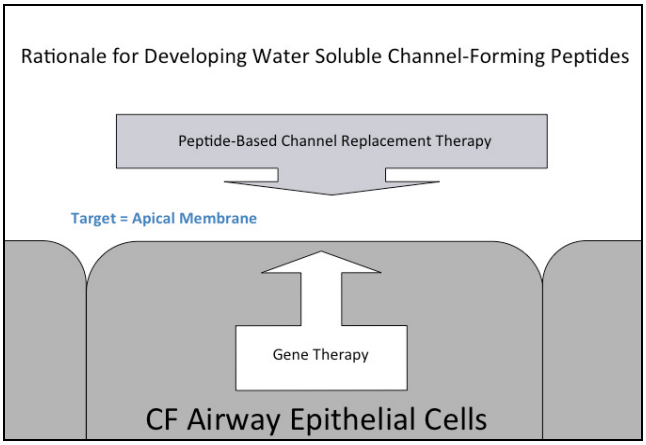

Fig. 1. The channel-forming peptide is delivered as an aerosol to the apical surface of CF airway cells. Upon binding to the surface it assembles to form an anion selective pathway to raise fluid secretion into the airway lumen thus rehydrating the airway surface fluid layer to allow proper cilia mediated airway clearance.

Class 1, the cys-loop ligand-gated ion channel superfamily of neurotransmitter receptors, includes the anion-selective inhibitory post-synaptic glycine (GlyR) and γ–aminobutyric acid type A (GABAAR) receptors, as well as cation selective nicotinic acetylcholine (nAChR), and 5-hydroxytryptamine type 3 (5-HT3R) receptors (Jensen et al., 2005; Sine and Engel, 2006) and the invertebrate post-synaptic glutamate receptor (Sunesen et al., 2006). These related structures all have a simple central pore defined by the parallel association of the second TM or 'M2' segments contributed by each of the five assembled subunits. Structural features common across members of this superfamily include the presence of heteropentameric bundles of subunits that are each composed of four hydrophobic TM segments, M1-M4, along with various sizes of intracellular and extracellular domains. Each M2 contributes a pore lining helix to form the channel. Unwin and co-workers (Unwin, 2003; Miyazawa et al., 2003; Unwin, 2005) published a 4 Å density map of the nAChR from *Torpedo marmorata*. The pentameric pore forms an hourglass-shaped pathway with the narrowest part at the middle of the lipid bilayer. The cation-conducting pathway, which is 40 Å long and extends beyond the lipid bilayer, is formed by parallel helices that are aligned, in registry, such that the same residues in different helices form rings that define discrete microenvironments. S266, E262, T244, E241, S248, and S252 form polar rings and hydrophobic residues V255 and L251 form the narrowest portion of the pore. It is important to note that in this barrel and stave type pore, amino acids possessing R-groups with a full charge are present. These negatively charged R groups are located as sites where the hourglass geometry is more open. McCammon and co-workers (Ivanov et al., 2007) modeled

the α1-GlyR pore by threading the GlyR M2 helical segments onto the Unwin structure. Then, using molecular dynamics, they simulated the water density profile and Cl^- translocation. A number of relevant conclusions were presented: the GlyR M2 pore is fully hydrated indicating that permeating Cl^- is fully hydrated as well, no hydrophobic barrier was observed that would help in dehydrating the anion, and that the pore at its narrowest had a radius of 2.5 Å. These observations are in agreement with data that we have observed with our anion selective pores, which will be presented later. The McCammon group did not take into account any contribution of the M1-M2 loop toward anion selectivity. This extracellular loop, through mutational analyses, has been implicated in selectivity by several groups (Gunthorpe and Lummis, 2001; Jensen et al., 2005).

Hilf and Dutzler (2008) published the first x-ray structure of a bacterial cys-loop channel at 3.3 Å resolution in a presumed "closed-state". This channel protein shares 16% sequence identity with the *Torpedo* nAChRα protein. It is strictly a cation channel although there is little selectivity between Na^+, K^+, and Ca^{2+}. It differs significantly from the mammalian cys-loop channels in that no helical cytoplasmic domain is present. The authors were unable to identify any ion binding sites within the pore itself. This structure is of great significance since it provides key parameters such as the handedness of the helical bundle (left) and the tilt angle of the helices. The TM pore-forming helix is 25 residues in length with the pore lined by residues S226, E229, T233, T236, T240, A243, Y247 and I251. This structure provides key spatial coordinates for our modeling studies.

GlyR α_1-subunits alone have been shown to form homopentameric channels, when expressed in *Xenopus* oocytes, with properties similar to the parent channels (Schmeiden et al., 1989). The ability of this channel to function as a homo-pentameric array made it an attractive candidate for probing ion selectivity and permeation.

Class 2 is represented by CFTR, the only channel member of the ABC transporter superfamily, which has 12 TM segments divided between two different halves each containing a nucleotide binding domain and linked by a regulatory domain (Riordan, 2008; Zhang et al., 2011). In a collaborative study with M. Montal, we identified four segments (M2, M6, M10, and M12) that assembled in synthetic bilayers to form a Cl^- conducting pore (Montal, et al., 1994). Since that time other TM segments (M1, M3, M5 and M11) have been implicated in participating in pore assembly (Zhang et al., 2000; Linsdell, 2006). Others have suggested that the active channel is composed of a homo-dimer (Zerhusen et al., 1999). The selectivity filter is believed to reside in the M6 segment (Zhou et al., 2002). Mutational studies in M6 support this assignment (Beck et al., 2008; Alexander et al., 2009). Clearly, this channel structure is more complex than that observed for the GlyR in that the CFTR pore requires the assembly of multiple non-identical TM segments.

Dawson and co-workers (Mansoura et al., 1998; Dawson et al., 1999; Smith et al., 2001; Liu et al., 2001) examined the selectivity properties of the CFTR channel, and proposed that reducing the dielectric of the pore is enough to cause anion selectivity. They prefaced their remarks by saying that the CFTR channel is probably a more primitive channel than the Class 1 channel types. CFTR exhibits lyotropic anion selectivity such that anions that are more readily dehydrated than Cl- are preferentially selected and show higher permeability rates. Their model predicts that larger anions, like SCN^-, although they experience weaker

interactions (relative to Cl^-) with water and the channel, are more permeant than Cl^- (but with a smaller conductance). They appear to have a smaller net energy cost entering the channel relative to that of Cl^-. That is, the reduced energy of hydration allows the net transfer energy (the well depth) to be more negative. The net positive charge of the pore lining residues also contributes to selectivity.

Class 3 is the ClC channel family, which includes ClC-0, through ClC-7 in vertebrate species. This is the only family for which detailed structural assignments have been generated. Several bacterial ClC channels have been crystallized and analyzed with regard to the pore structure and the Cl^- selectivity filter (Dutzler, et al., 2002; Dutzler et al., 2003). The active protein is a homo-dimer assembled from subunits that contain two identical anti-parallel domains. Each subunit contributes one channel to make a double-barreled channel structure. Each pore is made up of numerous anti-parallel helices of various lengths and contains two gating regions and a Cl^- binding site. More recent crystallographic and mutational data suggest that there are three anion-binding sites within the open state of each pore in the highly conserved ClC family of channels and transporters (Lobet and Dutzler, 2006). The proposed central selectivity filter is composed, in part, using amide nitrogens from three different helices (N, F and D) pointing toward the anion-binding site. These amides are more positively charged because of the helix dipoles. The site also contains S107 and T445 (Corry and Chung, 2006). The amides and hydroxyls of these atoms are oriented such that they could form hydrogen bonds with Cl^-. The serine side chain appears to be activated since the serine hydroxyl oxygen is also hydrogen bound to the amide nitrogen of I109. The anion never appears to interact with full positive charge from residues such as lysine or arginine. More recently three other residues have been implicated in selectivity through mutational studies K149, G352, and H401 in ClC-0 (Zhang et al., 2006). This class of channels is structurally distinct from the class 1 ligand-gated channels that contain a single pentameric array of parallel M2 helices of identical length. Despite these significant differences, the central ClC Cl^- selectivity filter offers insight into the types of binding interactions that are utilized by Cl^- selective channels.

4. M2GlyR studies

Early studies regarding first generation M2GlyR sequences When it became apparent that CFTR was a Cl^- selective channel, finding and inserting an alternative Cl^- conductive pathway into airway epithelia as a potential treatment modality became a realizable goal. Having already observed Cl^- selectivity in synthetic phospholipid bilayers (Reddy et al., 1993) with the M2 segment from the glycine receptor as both the free peptide (M2GlyR) and as a four-helix bundle (T_4-M2GlyR) built with a template strategy (Mutter et al., 1989; Iwamoto et al., 1994), this sequence was an obvious choice to begin studying its effects on epithelial monolayers. Due to the complexity of synthesizing and purifying the template sequence, the studies focused on the more tractable monomeric form.

The initial ion permeation studies in epithelial monolayers were conducted with the sequence PARVGLGITTVLTMTTQSSGSRA, corresponding to amino acids 250-272 in the glycine receptor protein, using confluent Madin-Darby canine kidney (MDCK) monolayers. When suspended at 100 μM in water containing 1% DMSO, the peptide caused a 1 μAcm^{-1} increase in short circuit current (I_{sc}), an extremely sensitive indicator of net ion flux. The increase in I_{SC}

occurred slowly with the net change being observed 30 minutes after peptide addition and this increase was observed only in 24 of 37 monolayers tested, suggesting inconsistencies in delivering the sequence to the membrane and then having it insert properly. In addition to the poor efficiency value, other drawbacks included limited solubility of the sequence and the inability to control the orientation of the inserted peptide in the bilayer.

To decrease these deficiencies, the M2GlyR sequence was modified systematically by adding up to six lysyl or diaminopropionic acid (DAP) residues to either the C- or N-terminus (Tomich et al., 1998). This study examined a number of physical, pharmacological and physiological characteristics of the adducted sequences. Increasing the positive charge at either terminus increased solubility dramatically and also directed the orientation of the peptide within the bilayer. The effect was more dramatic for the C-terminus additions (**Fig. 2**) with 5 lysines giving a peptide that showed solubility at saturation, in Ringer solution, of 56.1 mM. Placing four lysines at either the C- or N-terminus appeared to be optimal in that these modified sequences yielded larger I_{SC} values, greater aqueous solubility and exhibited nearly 100 percent efficiency in generating measurable changes in I_{SC}. The resulting I_{SC} was sensitive to bumetanide, a diuretic that blocks the activity of the $Na^+/K^+/2Cl^-$ cotransporter that is responsible for anion loading at the basolateral membrane, and to a non-selective Cl^- channel blocker, DPC. The aqueous solubility increased from 1.4 mM for the unmodified sequence to 27.5 and 13.4 mM for the CK_4- and NK_4-M2GlyR sequences, respectively. I_{SC} for CK_4- and NK_4-M2GlyR were larger by 2.7- and 1.2-fold, respectively.

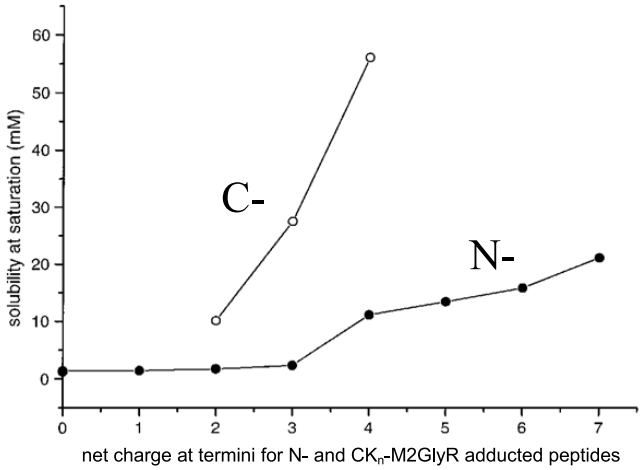

Fig. 2. Solubility as a function of net charge by the addition of lysines to either the C- or N-terminus of M2GlyR

Given the fact that adding lysines to either end improved solubility and showed increased magnitudes of net ion transport, studies were initiated to more fully describe the effects of CK_4-M2GlyR on MDCK cell monolayers primarily because placing lysines at the C-terminus yielded a pore that had an orientation, relative to the cell membrane, that was identical to the native GlyR channel. Additionally, the presence of the C-terminal lysines would be

expected to stabilize the helix dipole. The helix dipole is important in the packing of adjacent helices such as those found in the helical bundle formed by the supramolecular assembly of the M2 peptides.

CK_4-M2GlyR significantly increased I_{SC}, hyperpolarized transepithelial potential difference, and induced fluid secretion. In 28 monolayers, CK_4-M2GlyR (100 μM) significantly increased I_{SC} from 0.8 ± 0.1 to 3.3 ± 0.4 μAcm^{-2} and hyperpolarized transepithelial voltage (V_{te}) from 1.5 ± 0.4 to 3.5 ± 0.6 mV (apical bath negative). Transepithelial electrical resistance (R_{te}; a composite indicator of the transcellular and paracellular permeation pathways) decreased from 1,399 ± 341 to 1,013 ± 171 Ω cm^2. In other experiments the increase in I_{SC} was inhibited by bumetanide (100 μM) and by some Cl^- channel inhibitors. The effectiveness of the channel blockers followed the sequence niflumic acid ≥ 5-nitro-2- (3-phenylpropylamino) benzoate (NPPB) > diphenylamine-2-carboxylate (DPC) > glibenclamide. The effect of the peptide was not inhibited by 4,4'- diisothiocyanostilbene-2, 2'-disulfonic acid (DIDS). Removing Cl^- from the bathing solutions also abrogated the effect of the peptide. The Cl^- efflux pathway induced by CK_4-M2GlyR differs from the native adenosine 3', 5'-cyclic monophosphate (cAMP)-mediated pathway that can be activated by adrenergic agonists and by forskolin. First, intracellular cAMP levels were unaffected and second, the concentration of DPC required to inhibit the effect of the peptide was much lower than that needed to block the forskolin response (100 μM vs. 3 mM). These results support the hypothesis that the synthetic peptide, CK_4-M2GlyR, can form Cl^--selective channels in the apical membrane of secretory epithelial cells and can induce sustained transepithelial Cl^- secretion that can drive fluid secretion. I_{SC} remained relatively constant for the first 2 h after the addition of the peptide. After 3 h, the CK_4-M2GlyR-stimulated current was 90% of the current recorded at 60 min and decreased to 55% after 4 h. In washout experiments (n = 3), I_{SC} was measured after removing CK_4-M2GlyR from the bath. One hour after removal of the peptide, 39% of the CK_4-M2GlyR-induced current remained, and, after 2 h, there was no persisting effect of the peptide.

In a separate series of experiments (Wallace et al., 2000), transport of Cl^- through the CK_4-M2GlyR conductive pathway was modulated by basolateral K^+ efflux through Ca^{2+}-dependent K^+ channels. Application of CK_4-M2GlyR to the apical surface of T84 cell monolayers (derived from human colon) generated a sustained increase in I_{SC} and caused net fluid secretion. The current was reduced by clotrimazole, an inhibitor of SK and IK channels, and by charybdotoxin, a more selective and potent inhibitor of the *KCNN4* gene product, KCa3.1, a Ca^{2+}-dependent K^+ channel. Direct activation of these channels with 1-ethyl-2-benzimidazolinone (1-EBIO) greatly amplified the Cl^- secretory current induced by CK_4-M2GlyR. The effect of the combination of CK_4-M2GlyR and 1-EBIO on I_{SC} was significantly greater than the sum of the individual effects of the two compounds and was independent of cAMP. Treatment with 1-EBIO also increased the magnitude of fluid secretion induced by the peptide. The cooperative action of CK_4-M2GlyR and 1-EBIO on I_{SC} was attenuated by Cl^- transport inhibitors, by removing Cl^- from the bathing solution, and by basolateral treatment with K^+ channel blockers. These results indicate that apical membrane insertion of Cl^- channel-forming peptides such as CK_4-M2GlyR and direct activation of basolateral K^+ channels with benzimidazolones may coordinate the apical Cl^- conductance and the basolateral K^+ conductance, thereby providing a pharmacological approach to modulate Cl^- and fluid secretion by human epithelia deficient in CFTR.

Changes in the electrical properties of epithelial monolayers exposed to both 1-EBIO and CK_4-M2GlyR were observed. Basolateral addition of 1-EBIO (600 µM) induced a small increase in I_{SC} and doubled V_{te} with only a nominal decrease in R_{te}. Apical exposure of the 1-EBIO-treated monolayers to CK_4-M2GlyR (100 µM) caused an eight-fold increase in I_{SC} from 2.1 ± 0.2 to 16.5 ± 0.9 μAcm^{-2}, hyperpolarized V_{te} hyperpolarized by 7.3±0.5 mV and reduced R_{te} by 1.53±0.33 $K\Omega cm^2$. In two experiments, the response to 1-EBIO and CK_4-M2GlyR was monitored for 5 h. I_{SC} remained relatively constant during the first 60 min; however, I_{SC} had decreased to 73% of this current at 2 h, 53% at 3 h, 41% at 4 h and 29% of the current at 5 h. In washout experiments (n=2), the current generated by the additions of 1-EBIO and CK_4-M2GlyR was monitored for a set period of time, then CK_4-M2GlyR was washed out of the chamber. The removal of CK_4-M2GlyR from the medium decreased I_{SC} by 39%, whereas the subsequent removal of 1-EBIO decreased I_{SC} to the control level.

The addition of 1-EBIO increases the secretion of fluid induced by the apical application of CK_4-M2GlyR to T84 cell monolayers. T84 cell monolayers were grown in four groups of 10 monolayers, to test for the effects on the rate of transcellular fluid transport. Group I was incubated for 12 h in control medium, group II was exposed apically to CK_4-M2GlyR (500 µM), group III was exposed to 1-EBIO (300 µM) and group IV was exposed to both CK_4-M2GlyR and 1-EBIO. Monolayers incubated in control medium secreted fluid at a rate of 130 ± 40 $nLh^{-1}cm^{-2}$, a value that was not significantly different from monolayers exposed to 1-EBIO (180 ± 30 $nLh^{-1}cm^{-2}$). Monolayers exposed to just CK_4-M2GlyR exhibited a significantly greater rate of fluid secretion, 250 ± 20 $nLh^{-1}cm^{-2}$ and a combination of CK_4-M2GlyR and 1-EBIO increased the rate of fluid secretion further to 330 ± 20 $nLh^{-1}cm^{-2}$. These results demonstrated that anion secretion induced by the apical membrane insertion of CK_4-M2GlyR drives the secretion of fluid and that the direct activation of basolateral K^+ channels by 1-EBIO potentiates this effect on the rate of secretion.

In other experiments, it was determined that the increase in Cl^- and fluid secretion induced by combining CK_4-M2GlyR and 1-EBIO was independent of intracellular cAMP levels since the addition of the two compounds did not significantly affect cAMP content. This implies that CK_4-M2GlyR and 1-EBIO had minimal effect on CFTR Cl^- conductance or other cAMP-dependent processes. Therefore, we propose that the major action of 1-EBIO is to activate the Ca^{2+}-dependent K^+ channels and that the increase in the Cl^- secretory current is due to increasing the electrochemical driving force for Cl^- efflux through synthetic Cl^- channels generated by the membrane insertion of CK_4-M2GlyR. In summary, we have demonstrated that the synthetic Cl^- channel-forming peptide, CK_4-M2GlyR, induces Cl^- and fluid secretion by T84 cells, which are derived from human intestine. Activators and inhibitors of a basolateral Ca^{2+}-dependent K^+ conductance modulated the magnitude of this response. We propose that the combination of the novel synthetic Cl^- channel-forming peptide, CK_4-M2GlyR, and agents like 1-EBIO may have pharmacological benefits for inducing and modulating transepithelial Cl^- and fluid secretion independent of the cAMP-dependent Cl^- secretion that is impaired in CF.

In a subsequent study we examined whether CK_4-M2GlyR could exert effects on whole cell Cl^- conductance in isolated epithelial cells, and if the observed effects were the result of formation of a novel Cl^- conductance pathway, modulation of endogenous Cl^- channel activity, or a combination of these effects. The outcomes indicated that extracellular

application of CK_4-M2GlyR to isolated MDCK, T84, and IB3-1 cells resulted in increased permeability of the cells to Cl^-. The experimental evidence suggested a direct mechanism of action. Studies looking at the effects of the oligo-lysine portion of the sequence suggested that a poly-lysine modified K_4-helical peptide was not sufficient to activate endogenous CFTR through an electrostatic mechanism.

The ability of CK_4-M2GlyR to induce a time- and voltage-independent current in the IB3-1 cell line, which lacks functional CFTR, suggested that CK_4-M2GlyR does not increase Cl^- current by activating CFTR. Furthermore, the pharmacological profile of the induced current supports this conclusion. Specifically, the CK_4-M2GlyR-induced currents do not share biophysical characteristics of the hyperpolarization activated current associated with ClC-2 as determined with and without antisense ClC-2 cDNA, the swelling-activated current associated with Volume-Sensitive Organic Osmolyte/Anion Channels (VSOAC), with and without tamoxifen, and the Ca^{2+}-dependent Cl^- current activated by CaM Kinase II, with and without KN-62. Together, these results support the premise that the M2GlyR peptides increase I_{SC} across epithelial monolayers by forming a novel permeation pathway for Cl^- rather than by activation of endogenous Cl^- conductances.

In some of the most compelling work done to test the validity of the peptide-based channel replacement therapy, nasal potential difference (PD) studies were performed at the Gregory Fleming James Cystic Fibrosis Center at the University of Alabama, Birmingham, under the direction of Dr. Eric Sorscher. More than 40 mice were tested for effects of either CK_4-M2GlyR or NK_4-M2GlyR. A standardized protocol that employs transitions to amiloride, Cl^--free medium, and exposure to adrenergic stimuli was employed. The ΔF508 homozygous transgenic mouse nasal epithelia exhibit ion transport defects identical to those in CF human airways and, thus, are an excellent model to test for potential therapeutic effects. Ion transport was assessed by repeated nasal PD measurements in both transgenic and wild-type mice (Brady et al., 2001). Key data from a double-blind study employing both CK_4-M2GlyR and NK_4-M2GlyR are summarized in **Fig. 3**. As expected, isoproterenol, in a Cl^--free medium containing amiloride, caused a positive shift in nasal PD of CF mice (CF control) while causing a negative shift in the nasal PD of wild-type (WT) littermates. Importantly, following exposure of CF nasal epithelia to either CK_4-M2GlyR or NK_4-M2GlyR (500 μM) the effect of isoproterenol more closely resembled the effect in the WT animals than in the CF animals that received no peptide or were exposed to either of two control peptides that were expected to have no effect. Control #1 was too short to span the bilayer of a cell membrane and Control #2 (NK_4-Sc) has its transmembrane segment randomized, although computer modeling was employed to maximize helical propensities while minimizing the amphipathic character of the helix. Sustained Cl^- conductance was observed for up to 6 h after a single application of peptide in solution. While this outcome is very encouraging, this type of treatment would have to be administered one or more times per day for optimal clinical results.

Concurrent exposure to 1-EBIO changed the direction for the development of M2GlyR channel-forming peptides. Initially, most studies were performed using CK_4-M2GlyR. However, CK_4-M2GlyR and NK_4-M2GlyR behaved differently in the presence of the K^+-channel opener. N-terminal modification of a channel-forming peptide increases capacity for epithelial anion secretion. In Ussing chamber experiments, apical exposure of MDCK and T84 cell monolayers to NK_4-M2GlyR (250 μM) increased I_{SC} by 7.7 ± 1.7 and 10.6 ± 0.9 μAcm$^-$

^{2}, respectively (Broughman et al., 2001). These values are significantly greater than those previously reported for the same peptide modified by adding the lysines at the C- terminus (Wallace et al., 1997). NK_4-M2GlyR caused a concentration-dependent increase in I_{SC} ($k_{1/2}$ = 190 μM) that was potentiated two- to threefold by 1-EBIO (300 μM). NK_4-M2GlyR-mediated increases in I_{SC} were insensitive to changes in apical cation species. Pharmacological inhibitors of endogenous Cl^- conductances (glibenclamide, DPC, NPPB, DIDS, and niflumic acid) had little effect on NK_4-M2GlyR-mediated I_{SC}. Whole cell membrane patch-voltage clamp studies revealed an NK_4-M2GlyR-induced anion conductance that exhibited modest outward rectification and modest time- and voltage-dependent activation. Planar lipid bilayer studies indicated that NK_4-M2GlyR forms a 50-pS anion conductance with a $k_{1/2}$ for Cl^- of 290 mEq. NK_4-M2GlyR was similar to the previously characterized analog, CK_4-M2GlyR, in that both sequences elicited increases in the anion-selective current in lipid bilayers, whole cell membrane patches, and epithelial monolayers. When employed at similar concentrations, NK_4-M2GlyR provided for greater anion secretion across epithelial cell monolayers than any related channel-forming peptide tested to this point. Effects for NK_4-M2GlyR were observed with as little as 25–30 μM, and maximal effects were observed with about 500 μM (**Table 1** and **Fig. 4**; Broughman et al., 2002a).

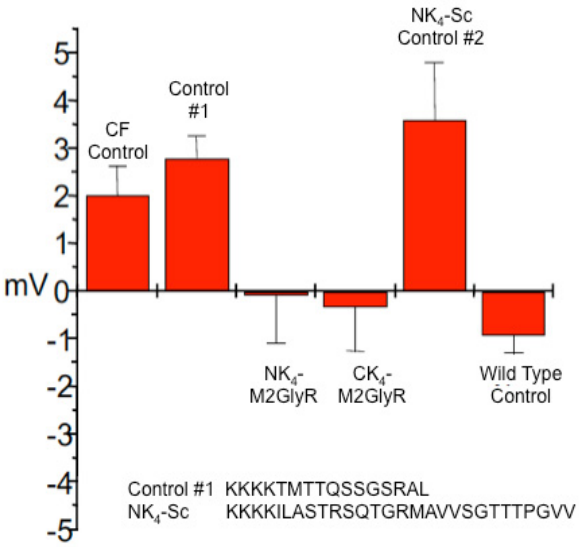

Fig. 3. Isoproterenol-induced change in nasal PD of ΔF508 homozygous mice and wild-type littermates in the absence or presence of indicated peptides.

Sequence	name	Mr (Da)	Sol.(mM)	n	I_{MAX} (μA/cm2)	$k_{1/2}$ (μM)
1. PARVGLGITTVLTMTTQSSGSRA	M2GlyR	2304.7	1.4	N/A	N/A	N/A
2. PARVGLGITTVLTMTTQSSGSRAKKKK	CK_4-M2GlyR	2817.4	27.5	2.7 ± 0.9	102.5	>500
3. KKKKPARVGLGITTVLTMTTQSSGSRA	NK_4-M2GlyR	2817.4	13.4	1.52 ± 0.55	24.3 ± 0.5	319 ± 192

Table 1. Characterization of M2GlyR peptides with C- and N-terminal oligo-lysine adducts.

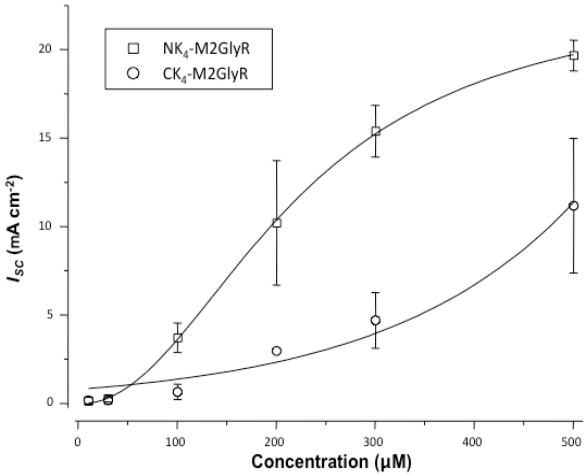

Fig. 4. The dependence of I_{SC} of MDCK monolayers on NK_4-M2GlyR and CK_4-M2GlyR concentration in the presence of 1-EBIO. Solid lines represent the best fit of a modified Hill equation to the data sets.

The resulting parameters for NK_4-M2GlyR (I_{max} = 25.2 ± 10.4 μAcm^{-2}, $k_{1/2}$ = 319 ± 192 μM, n (Hill coefficient) = 1.52 ± 0.55) are similar to those reported above , I_{max} = 24.3 ± 0.5 μAcm^{-2}, $k_{1/2}$ = 208 ± 6 μM, and n = 2.6 ± 0.1). This degree of cooperativity suggests that a multi-step process is required to form functional channel assemblies. Whether the cooperative step involves membrane partitioning, assembly of the helical bundles into structures, or a combination of these necessary steps for channel formation is not known. The concentration dependence of CK_4-M2GlyR is right-shifted compared to that of NK_4-M2GlyR, with the response at the greatest concentration tested (500 μM) showing no indication of saturation. The experimental data for CK_4-M2GlyR, when fitted by the modified Hill equation, resulted in a substantially greater value for I_{max} than that observed for a variety of agonists and pore-forming peptides (25–30 μA cm^{-2}). When employed at similar concentrations, NK_4-M2GlyR provides for greater anion secretion across epithelial cell monolayers than any related channel-forming peptide tested thus far. These results indicate that NK_4-M2GlyR forms an anion-selective channel in epithelial monolayers and again showed its therapeutic potential for the treatment of hyposecretory disorders such as CF.

One of the early applications of NK_4-M2GlyR included a study looking at the effect of exogenously applied peptide to the surface of immortalized human tracheal epithelial cells from a homozygous ΔF508 CFTR CF patient (Yankaskas et al., 1993). CF is characterized by defective epithelial Cl^- transport with damage to the lungs occurring, in part, via chronic inflammation and oxidative stress. Glutathione, a major antioxidant in the airway lining fluid, is decreased in CF airway due to reduced glutathione efflux (Gao et al., 1999). This observation prompted a study to examine the question of whether exposure to channel-forming peptides would also restore glutathione secretion (Gao et al., 2001). Addition of the Cl^- channel-forming NK_4-M2GlyR (500 μM) and a K^+ channel activator (chlorzoxazone, 500 μM) increased Cl^- secretion, measured as bumetanide-sensitive I_{SC}, and/or glutathione

efflux, measured by high-performance liquid chromatography, in a human CF airway epithelial cell line (CFT1). Addition of the peptide alone increased glutathione secretion (181 ± 8% of the control value), whereas chlorzoxazone alone did not significantly affect glutathione efflux; however, chlorzoxazone potentiated the effect of the NK_4-M2GlyR on glutathione release (359 ± 16% of the control value). CK_4-M2GlyR has decreased efficacy compared with NK_4-M2GlyR in both I_{SC} and GSH efflux assays. The addition of 1-EBIO also amplified the effect of NK_4-M2GlyR (500 μM) on GSH efflux (286 ± 1 % of control values). These studies demonstrated that glutathione efflux can be modulated by channel-forming peptides and is likely associated with Cl^- secretion, not necessarily with CFTR per se, and the defect of glutathione efflux in CF can be overcome pharmacologically.

Both orientations of the M2GlyR helix within the membrane form anion-selective pores. However, differences in solubility, solution associations and channel-forming activity for the oligo-lysyl adducted forms were observed. While deciding on which of the oligo-lysine adducted M2GlyR peptides to develop further, we began a study utilizing chemical cross-linking, NMR and molecular modeling to determine how the positioning of the lysyl residues affected the channel properties and structural characteristics. These sequences are amphipaths with distinct clusters of hydrophobic and hydrophilic residues. In aqueous solution, hydrophobic patches associate and hydrophilic ones are solvent exposed. This property generally leads to aggregation through a concentration dependent process. This model predicts that multiple higher molecular weight assemblies, which do not readily interact with membranes, would be formed (**Fig. 5**). Evidence indicating aggregate formation is discussed below. A preferred outcome, however, would be to have a peptide that remained predominantly monomeric in solution while retaining its membrane binding and insertion activities. The actual sequence of insertion and assembly events leading to a functional channel are still unresolved. We do know that much of the process is slowly reversible based on perfusion washout experiments (indicated by the double ended arrows). Two possible routes are shown. One (right) has the peptide inserting and folding as a single step followed by assembly. The second (left) has peptide folding occurring at the surface followed by assembly as a prerequisite for insertion. A mixture of the two pathways could also be possible. Optimization of the channel-forming structure included modifications to reduce solution oligomerization and thereby increase the concentration of peptide that could insert and form active assemblies. CK_4-M2GlyR and NK_4-M2GlyR formed aggregates in aqueous solutions to differing degrees, as shown in **Fig. 6**. A cross-linking reagent was used to trap solution aggregates that were visualized using sodium dodecyl sulfate – polyacrylamine gel electrophoresis (SDS-PAGE) (Broughman et al., 2002b). Bis [Sulfosuccinimidyl] suberate (BS^3), a water-soluble homo-bifunctional cross-linking reagent that reacts with free amino groups in the lysine adducts was employed. The cross-linking reactions were carried out in 10 mM 4-(2-hydroxyethyl) piperazine-1-ethanesulfonic acid (HEPES) buffer, pH 6.5, at selected peptide concentrations in the presence of a 40-fold molar excess of cross-linking reagent. The results from a typical experiment are shown in **Fig. 6**. Lanes 5 and 9, show the electrophoretic mobility of non-cross-linked CK_4-M2GlyR and NK_4-M2GlyR boiled in 10% SDS, respectively. Under these conditions both sequences are monomeric, indicating that the solution associations that are trapped with the cross-linking reagent (in the adjoining lanes) are dissociated in the presence of the anionic detergent. The cross-linked molecular weight profiles for the two sequences are strikingly different. CK_4-M2GlyR forms lower molecular weight associations with monomer through trimer being

the most prevalent. NK_4-M2GlyR forms many more associated forms, starting with monomer and going beyond 20-mers. Comparing the relative concentration of monomer to the higher species for each of the sequences, monomer is the most abundant species for CK_4-M2GlyR while in NK_4-M2GlyR the monomer accounts for less than 50% of the captured species. This result was somewhat surprising since NK_4-M2GlyR has considerably more activity per peptide concentration even though there is apparently a smaller percentage of monomer able to bind and insert into the membrane.

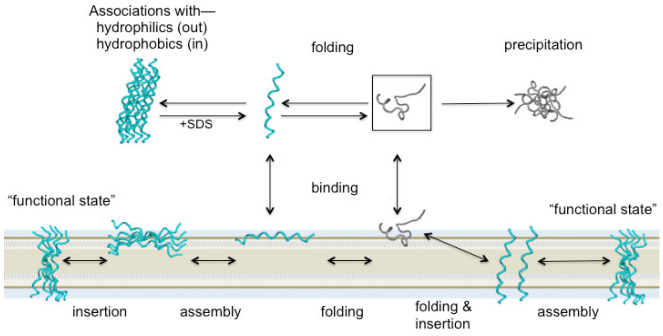

Fig. 5. Solution and membrane inserted states for channel-forming peptides.

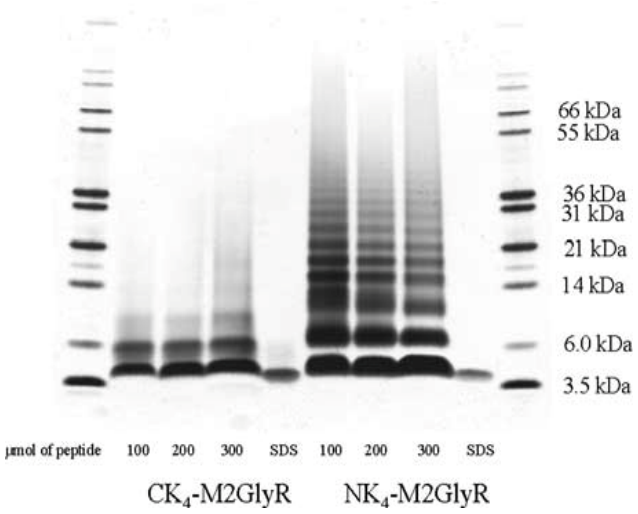

Fig. 6. Silver-stained polyacrylamide gel of cross-linked NK_4-M2GlyR and CK_4-M2GlyR.

Assuming that the energy barrier for the translocation of the four-lysyl residues across the hydrophobic membrane is prohibitive (Vogt et al., 2000), either orientation (NH_2 or COOH terminal towards extracellular surface) can insert into the membrane and assemble into an anion-conducting pore. However, based on the observation that the concentration required to produce 50% of the maximum increase in I_{SC} ($k_{½}$) for NK_4-M2GlyR is one-third less than that required for CK_4-M2GlyR (319 μM vs. 553 μM, respectively), the efficiency of the

insertion or the assembly of these two peptides into channel-forming structures is not equivalent. Furthermore, the concentration-dependent effects of the peptides on I_{SC} show a smaller Hill coefficient for NK_4-M2GlyR than CK_4-M2GlyR (n = 1.5 vs. 2.3, respectively). This suggests that one or more of the steps required for channel assembly (e.g., insertion, oligomerization) is/are more cooperative in the case of CK_4-M2GlyR. Alternatively, as NK_4-M2GlyR is less soluble than CK_4-M2GlyR in aqueous solution, the hydrophobic driving force for the insertion of NK_4-M2GlyR into the membrane is greater. In either case, structural differences between the lysine-modified peptides result in altered channel-forming activity.

A series of one- and two-dimensional NMR experiments were performed on NK_4- and CK_4-M2GlyR. TOCSY NMR spectra were recorded for each (Broughman et al., 2002b). Data presented in **Fig. 7** show the fingerprint region (NH to Cα and side chain proton connectivity) for 500 MHz 1H 2D-experiments for both peptides recorded in water containing 30% deuterated trifluoroethanol (TFE) at 30°C (assignments are shown for the lysine residues). The extent of chemical-shift dispersion of the backbone proton resonances, particularly of the lysine residue amide protons (in spite of the oligomeric nature of the lysines in these sequences), suggest that such a spread of chemical shift can be induced only by secondary structure. However, in comparing the chemical shifts for the lysine residues in the two TOCSY spectra, it is clear that the environments for these basic amino acids in the two peptides are distinct. For the NH_2-terminal lysine adducted peptide the dispersion range of the TOCSY chemical shifts for 3 of the 4 lysines was 8.55 to 8.1 ppm. The fourth lysine could not be assigned. In contrast, the COOH-terminal-adducted peptide had a dispersion range of chemical shifts that spanned 8.15–7.72 ppm. All four of the CK_4-M2GlyR lysine resonances were assigned. Greater dispersion in the chemical shift pattern observed with NK_4-M2GlyR indicates that these residues are more mobile and solvent exposed while the lysine residues adducted to the COOH-terminus are hydrogen bonded intramolcularly.

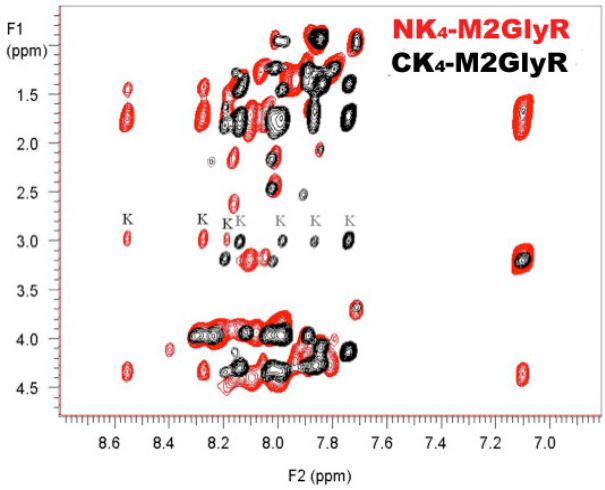

Fig. 7. TOCSY NMR spectra (500 MHz) of NK4-M2GlyR and CK4-M2GlyR.

The NMR coordinates for CK_4-M2GlyR and NK_4-M2GlyR were modeled using a combination of energy based minimizations and molecular-dynamics simulations. The lysine residues of CK_4-M2GlyR form a C-cap by extensive H-bonding interactions with the helix backbone, which remain fairly static throughout the molecular dynamics simulation period. The side chain ε-amino group of K24 of CK_4-M2GlyR forms a capping structure that stabilizes the helix by forming H-bonds with the backbone carbonyl groups of S21, R22 and A23, fulfilling H-bonding interactions that are absent in the COOH terminal residues of an α-helix. The ε-amino group of K25 of CK_4-M2GlyR forms H-bonds with the backbone carbonyl groups of T16 and K-27 and the hydroxyl side chain of T16. The ε-amino groups of K26 and K27 of CK_4-M2GlyR form hydrogen bonds to the backbone carbonyl of K25 and the side chain carbonyl of Q17, respectively. The side chain ε-amino groups of K1 and K4 of NK_4-M2GlyR do not form H-bonds, as the lysyl residues' side chains extend away from the helix backbone. There was very little motion of the helix backbone of CK_4-M2GlyR during the simulation period. In contrast, the lysine residues of NK_4-M2GlyR remained mostly extended away from the helix during the simulation, interacting minimally with the M2GlyR backbone. These differences in dynamics could affect the rates of assembly and pore geometries. Large differences are predicted for the dipoles of NK_4-M2GlyR and CK_4-M2GlyR (**Fig. 8** left and right structures, respectively). Note the similarities, both in magnitude and in orientation, between the dipoles of the unmodified M2GlyR sequence and NK_4-M2GlyR. The dipole of CK_4-M2GlyR is shifted by nearly 90 degrees and is less than 2% of the magnitude of the dipole for the parent compound. This perturbation of the dipole could play a role in the differences observed in peptide-peptide association and channel activity of the CK_4-M2GlyR peptide.

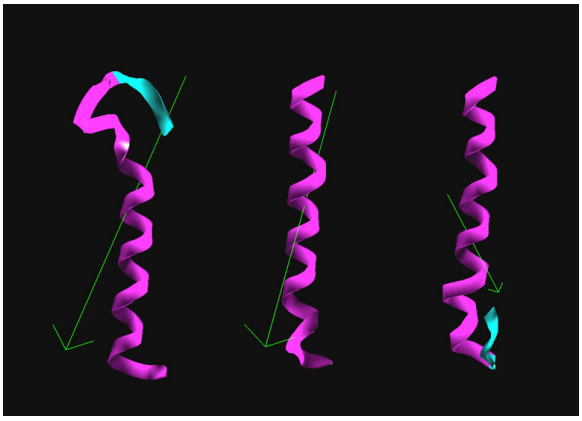

Fig. 8. The dipole moments of NK_4-M2GlyR (left), M2GlyR (center) and CK_4-M2GlyR (right) are shown as ribbon structures (magenta is helix and cyan is random coil) with the dipoles represented by green arrows. For this representation, the dipoles of NK_4-M2GlyR and M2GlyR were scaled down by a factor of 20, while the dipole for CK_4-M2GlyR was scaled up by a factor of 3.

To identify the portion of the M2GlyR molecule that was promoting the solution assemblies of NK_4-M2GlyR, channel activity and cross-linking experiments were performed on various truncated forms of CK_4-M2GlyR and NK_4-M2GlyR. The results (**Figs. 9 and 10**) suggested that

a nucleation site for self-association of the peptide is located near the COOH-terminus of the M2GlyR sequence since removal of five residues (SGSRA) from the C-terminus of NK_4-M2GlyR resulted in a reduction of higher molecular weight species. Importantly, there was little loss of ion transport activity. Removal of additional C-terminal residues led to a progressive decrease in I_{SC}, although there was a slight reduction in apparent solubility to 11.1 mM. Measurable activity was observed with even 11 residues removed from the C-terminus. In contrast, the nucleation site is likely masked by the oligo-lysine tail at the COOH-terminus, which prevents formation of higher order assemblies by CK_4-M2GlyR and removal of residues from the N-terminus of CK_4-M2GlyR had little effect on the various low molecular weight associations. However, these truncated forms exhibited substantially less ion transport activity. The truncated NK_4 sequence, referred to as NK_4-M2GlyR-p22, became the lead compound for further development. Removing the five residues greatly reduced the cost of synthesizing a purer peptide with fewer failed sequences.

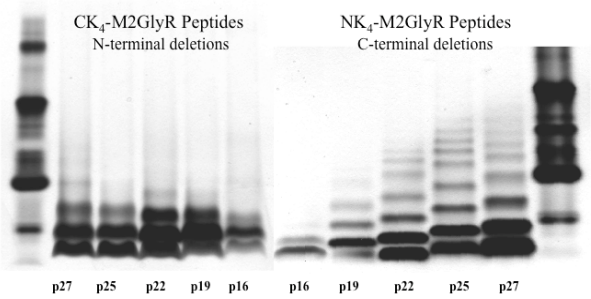

Fig. 9. Silver-stained Tricine polyacrylamide gel of cross-linking patterns for truncated CK_4-M2GlyR and NK_4-M2GlyR treated with a 40-fold excess of crosslinking reagent.

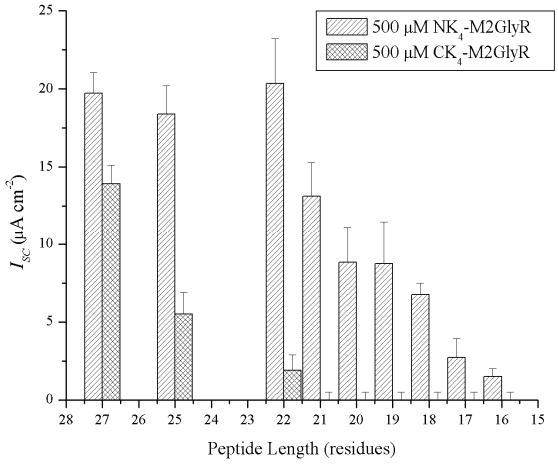

Fig. 10. I_{SC} induced by the full length and truncated NK_4-M2GlyR and CK_4-M2GlyR peptides (500 μM) on MDCK epithelial monolayers. Symbols represent the mean and standard error of three to seven observations.

Results described thus far indicate that the native M2 sequence that forms the GlyR pore can be employed to form de novo anion selective channels in epithelial cell membranes. Further, the structure can be optimized to enhance aqueous solubility and to decrease solution aggregation, which increases effective bioavailable concentration. Lysyl-adduction at the amino terminus appeared to be preferred based upon outcomes with truncated peptides. An additional and exciting outcome of these truncation studies was that shorter peptides might be used to achieve the therapeutic goal, which provides for many potential benefits in design and delivery of this therapeutic modality.

Studies on the second generation of NK_4-M2GlyR-p22 sequences In the process of truncating the NK_4-adducted M2GlyR sequence, a number of hydrophilic residues were eliminated as defined by the Wimley and White hydrophobicity scales developed for TM sequences (Wimley and White, 1996; Wimley and White, 1999; Wimley and White, 2000; Jayasinghe et al., 2001). The increase in hydrophobicity was reflected in reduced solubility for the deletion peptides. Among the residues removed was R22 in the C-terminus of the parent M2 sequence. It has been postulated, based on solution NMR studies in dodecyl phosphatidylcholine micelles, that the registry of the wild-type TM segment is defined by residues R3 and R22, thereby defining an 18-residue TM segment (Tang et al., 2002; Yushmanov et al., 2003). Arginine is often located at the water/lipid interface in TM segments (Vogt et al., 2000; Harzel and Bechinger, 2000; Mitaku et al., 2002). Without the C-terminal R in the NK_4-M2GlyR-p22 sequence, both ion selectivity and positioning, and registry of the TM segment within the acyl lipid core are potentially compromised. Therefore, a study was initiated to evaluate the effects on channel transport properties of reintroducing an R at positions near the new carboxyl-terminus. Arginine residues were introduced individually at positions 18 through 22 and in subsequent experiments double amino acid replacements were generated with aromatic amino acids placed at or near the C-terminus along with R at positions 19-22. MDCK monolayers were used to assess peptide-dependent ion transport.

A series of five individual C-terminal R substitutions were made placing R at the following positions: M18R, T19R, T20R, Q21R and S22R (Shank et al., 2006). With the exception of M18R, the substituted peptides generally exhibited similar concentration dependent I_{SC} profiles in MDCK monolayers (**Table 2**). Substitution of an R enhanced solubility by 50% or more, did not affect the Hill coefficient (**n**), showed similar half maximal activity ($k_{1/2}$) values and had similar helical content as judged by circular dichroism recorded using 50 μM peptide in 10 mM sodium dodecyl sulfate (SDS). Cross-linking experiments using BS^3 revealed that all of these substituted sequences showed solution aggregation patterns similar to that seen for NK_4-M2GlyR-p22 (e.g., see **Fig. 9**).

Rather than rely simply on an R to define the lipid-water boundary at the truncated end of M2GlyR, a W was used to replace the C-terminal serine. A propensity for tryptophans residing at the aqueous/lipid interface also had been observed and tested by others (Braun and von Heijne, 1999; Mall et al., 2000; Demmers et al., 2001; de Planque et al., 2003; Granseth et al., 2005; van der Wel et al., 2007; Hong et al., 2007). Placing a W at the C-terminus sets the registry of the TM segment that spans the bilayer. In the absence of an R or aromatic residue at or near the C-terminus, the peptide could rise up and down within the fluid bilayer thereby affecting the depth of peptide insertion into the membrane and tilt angle of the peptide. By limiting mobility, the degrees of freedom for the TM registry of the

peptide are reduced. During the assembly process this allows the annealing peptides to find their preferred interfacial contacts faster and at a lower concentration. **Fig. 11** shows the concentration dependence on I_{SC} for the full length and the truncated M2GlyR peptides when applied to the apical membrane of MDCK cells in the presence of 1-EBIO (Cook et al., 2004). The solid lines represent the best fit of a modified Hill equation to each data set. In paired monolayers both NK_4-M2GlyR-p27 and NK_4-M2GlyR-p22 peptides (previously characterized in Broughman et al., 2002a) displayed similar concentration dependency curves and induced similar I_{SC} at each concentration tested. Introduction of the W in NK_4-M2GlyR-p22 S22W yielded a curve with a reduced I_{MAX} (13.0 ± 1.0 μAcm^{-2}) but more importantly a significantly reduced $k_{1/2}$ (44 ± 6 μM) with a considerably greater Hill coefficient of 5.4 ± 2.9. The sum effect of changes in the three kinetic parameters (I_{MAX}, $k_{1/2}$, and Hill coefficient) is a substantial reduction in the peptide concentration required to yield maximal anion secretion.

Sequence	Substitution	Mr (Da)	Sol.(mM)	n	I_{MAX} (μA/cm^2)	$k_{1/2}$ (μM)
1. KKKKPARVGLGITTVLTMTTQS	none	2358.9	11.1	1.9 ± 0.6	23.7 ± 5.6	210 ± 70
2. KKKKPARVGLGITTVLTMTTQR	S22R	2427.9	15.6	2.7 ± 0.9	24.1 ± 5.3	290 ± 60
3. KKKKPARVGLGITTVLTMTTRS	Q21R	2387.0	19.7	2.2 ± 1.1	31.0 ± 18.0	390 ± 220
4. KKKKPARVGLGITTVLTMTRQS	T20R	2414.0	18.7	1.3 ± 0.5	28.5 ± 14.8	310 ± 227
5. KKKKPARVGLGITTVLTMRTQS	T19R	2414.0	18.3	0.7 ± 0.6	16.3 ± 3.5	120 ± 40
6. KKKKPARVGLGITTVLTRTTQS	M18R	2383.9	23.3	0.6 ± 2.6	3.0 ± 4.0	840 ± 200

Table 2. Characterization of M2GlyR-p22 derived peptides with C-terminal Arginines.

We then assessed the solution associations of the selected NK_4-M2GlyR peptides using a silver-stained gel following cross-linking reactions. In **Fig. 12**, lane 1 (consistent with 34:9-11) contained a mobility standard to indicate relative molecular weights. Lanes 2 through 9 contain the indicated peptides that were suspended in aqueous buffer in the absence and presence of a twenty-fold excess of BS3, as indicated The cross-linker revealed the presence of higher molecular weight homo-oligomers. Without the addition of cross-linker and after boiling the sample in SDS containing loading buffer, only monomer was observed. The W substituted sequence, however, appeared to be predominantly monomeric in solution under either experimental condition. These results indicated that NK_4-M2GlyR-p22 S22W (150 μM) forms essentially no aggregates in aqueous solution and the entire suspended mass is capable of membrane interaction.

It is unclear whether the left shift in $k_{½}$ observed for the W containing peptide in **Fig. 11** is due solely to an increase in concentration of the membrane active monomeric species or includes a contribution from the C-terminal W limiting the possible orientations of the peptide within the bilayer. The change in the Hill coefficient is likely due to the addition of the membrane anchor that facilitates the supramolecular assembly of the peptides into an active oligomeric pore. We speculated that the anchor reduces the degrees of freedom for

the TM segment making alignment more favorable during assembly. An alternative explanation could be that in the absence of the tryptophan there is both positive and negative cooperativity. Addition of the tryptophan eliminates the negative cooperativity and we see the level of positive cooperativity that might be expected for the assembly of a pentameric structure. The presence of the fluorescent tryptophan also provides both a convenient method for determining the concentration of the peptide solution and a sensitive tool for probing the environment surrounding the indole.

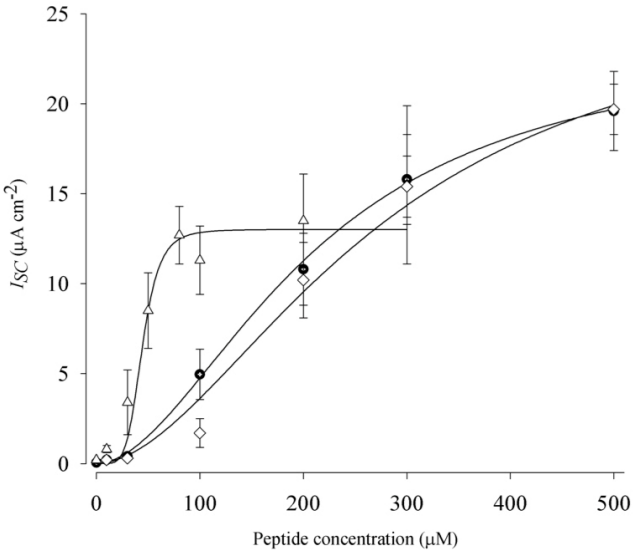

Fig. 11. Concentration-dependence of I_{SC} induced by NK_4-M2GlyR derived peptides on MDCK epithelial monolayers. The NK_4-M2GlyR derived peptides concentration dependent I_{SC} curves are as follows: NK_4-M2GlyR p27(◊), NK_4-M2GlyR p22 WT (●) and NK_4-M2GlyR p22 S22W (Δ).

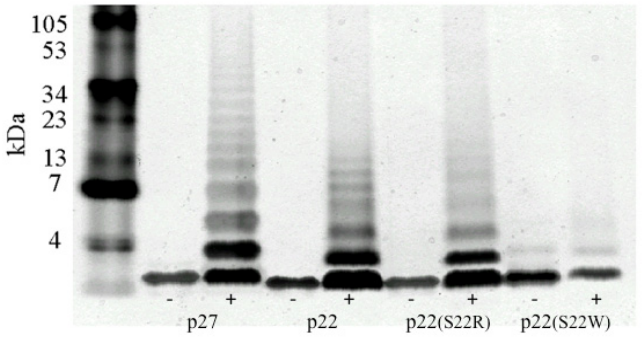

Fig. 12. NK_4-M2GlyR and derivative peptide solutions (150 μM) mixed without (**-**) and with (**+**) a 20-fold excess of BS^3 cross-linker.

NMR structural and computer modeling studies were carried out on 40% deuterated TFE solutions of NK_4-M2GlyR-p22 and NK_4-M2GlyR-p22 S22W to determine how the substituted C-terminal W potentially influences solution associations of the peptide (Cook et al., 2004). A measurement of the NK_4-M2GlyR-p22 (WT) peptide structure shows that the length of the entire TM segment is greater than 32 Å, more than enough to span the hydrophobic core of the membrane (**Fig. 13,** left structure). This structure is similar to the results shown in micelle studies done on the wild-type glycine receptor α_1 subunit (Tang et al., 2002; Yushmanov et al., 2003). An identical segment of the peptide was determined to be helical when incorporated in SDS micelles. The rest of the peptide was unstructured and flexible, including the C-terminus. The outcomes indicated that the structured portion of the peptide is restricted to residues 8 to 22 regardless of the length of the peptide. The WT structure resembles other TM segments observed in the x-ray crystal structure of a ClC chloride channel. In that structure, the Cl^- binding TM segments are made up of shorter helices that do not completely span the width of the membrane (Dutzler et al., 2002; Esrévez and Jentsch, 2002).

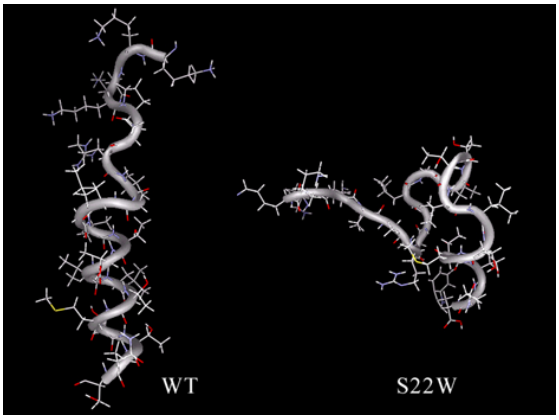

Fig. 13. Calculated models of NK_4-M2GlyR-p22 and NK_4-M2GlyR-p22 S22W in TFE.

The structured C-terminus of NK_4-M2GlyR-p22 S22W is made up of a single-turn helix (residues 11 - 14), a stretched beta-like turn (residues 14 - 17), and then another two-turn helix (residues 15 - 21). The observed structure indicated a helical content of about 40%, which was in good agreement with CD data for the S22W containing 22-residue peptide. This backbone structure allows the peptide to loop or fold over into a closed structure (**Fig. 13**). This fold sequesters the hydrophobic residues such that the acyl side chains have reduced solvent exposure. The structure likely has little relevance to a TM segment where the aliphatic side chains would be fully exposed and interacting with the lipid acyl chains in the membrane bilayer. Nonetheless, the C-terminal fold of NK_4-M2GlyR-p22 S22W explains why the peptide remains in the monomeric form in solution, since the hydrophobic groups are less exposed and unable to associate with hydrophobic groups from other peptides. While TFE is not added to peptide stock solutions used for assessing channel activity, it is clear that this monomer-inducing fold is sampled with enough frequency that the higher molecular weight forms do not occur. Based on the CD spectra obtained using 10 mM SDS micelles, the peptide is able to adopt a more helical structure, much like the WT peptide.

NMR studies in SDS (**Fig. 14**) confirmed the CD results (Herrera et al., 2010). These atomic structures clearly show that both NK_4-M2GlyR-p22 (WT) and NK_4-M2GlyR-p22 S22W are linear and mostly helical from residues 6–20 in SDS micelles. The N-terminal lysines are largely unstructured and apparently exhibit substantial flexibility. These lysine residues are expected to be out of the micelle floating in the aqueous environment and/or interacting with the sulfate groups. The hydrophobic and hydrophilic side chains are segregated to different sides of the helix, as expected for channel forming TM segments.

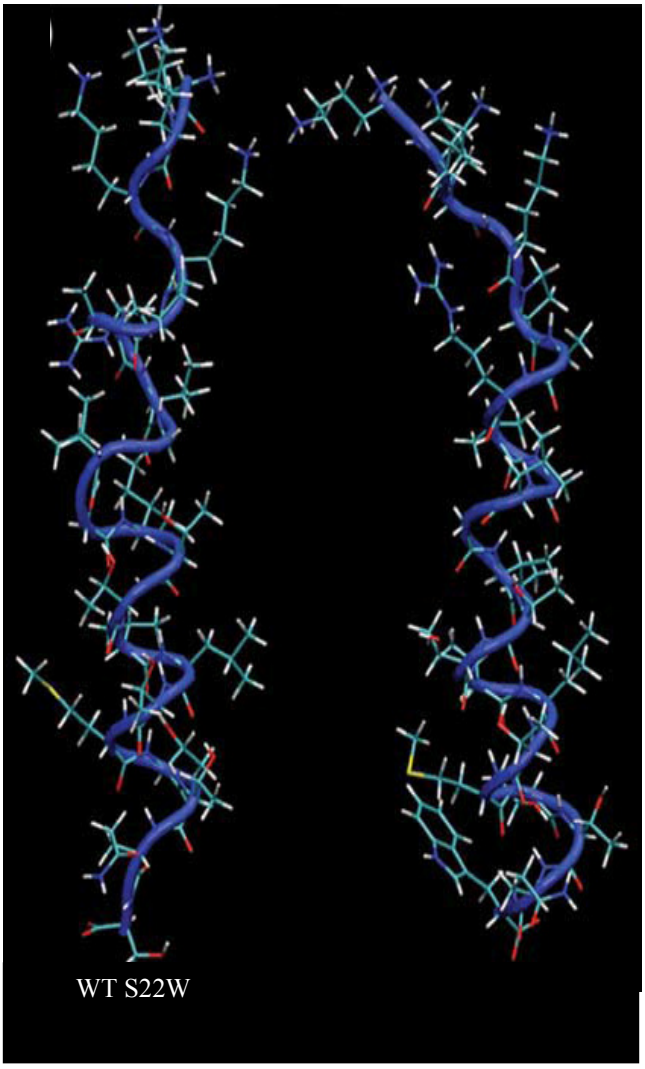

Fig. 14. Average structures of NK_4-M2GlyR-p22 and NK_4-M2GlyR-p22 S22W after MD refinement in an implicit membrane. Backbones are shown as a blue tube with licorice side chains.

NMR structures, along with a range of additional experimental data and theoretical considerations, were utilized to assemble the monomer structure into channels, including oligomerization state, pore-lining interface, helix packing distance, and tilt angle. In particular, experimental identification of the pore-lining residues greatly reduces uncertainty of the channel assembly and allows the construction of reliable initial structural models. All-atom molecular dynamics (MD) simulations in fully solvated 1-palmitoyl-2-oleoyl-*sn*-glycero-3-phosphocholine (POPC) bilayers were subsequently carried out to refine these structural models and to characterize and validate the structural and dynamical properties of the channels (**Fig. 15**). The results demonstrate that the channel structures as constructed are adequately stable within the simulation time frame (up to 20 ns) and remain sufficiently open for ion conductance. All initial structures relax to transiently stable structures within a few nanoseconds. Analysis of the relaxed structures of NK_4-M2GlyR-p22 WT and NK_4-M2GlyR-p22 S22W reveal important differences in their structural and dynamical properties, providing a basis for understanding the differences in channel activities. Specifically, the structural characterization supports the initial postulation that the S22W substitution in NK_4-M2GlyR-p22 helps to anchor the peptide in the membrane and reduces the flexibility of the whole assembly. The implied increased stability of the NK_4-M2GlyR-p22 S22W channel potentially explains the steeper short circuit current-concentration slope measured experimentally. Furthermore, introduction of the C-terminal W appears to lead to global changes of the channel structure. The NK_4-M2GlyR-p22 S22W channel maintains a smaller opening at the narrowest region and throughout the rest of the pore compared with the NK_4-M2GlyR-p22 channel. The smaller size of NK_4-M2GlyR-p22 S22W could effectively reduce its ion throughput or conductance by a magnitude that is consistent with a nearly 50% reduction in measured I_{MAX}. The ability to recapitulate these differences in key physiological properties observed experimentally is an important validation of the proposed structural models.

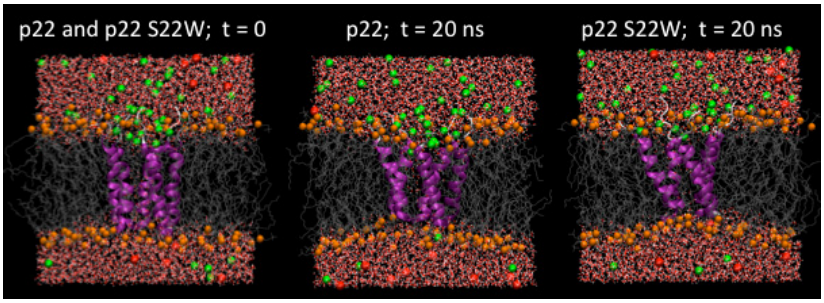

Fig. 15. Snapshots of NK_4-M2GlyR-p22 and NK_4-M2GlyR-p22 S22W left-handed channels in a fully solvated POPC bilayer before and after the 20 ns production simulation. Both peptides have identical structures at t = 0.The protein is shown in purple cartoon and lipid molecules shown in the grey licorice with phosphorus atoms shown as orange spheres.

Development of third generation NK_4-M2GlyR-p22 derived sequences From a drug delivery perspective, adding the W at the C-terminus yields a compound that can be delivered from solution at a stable accurate concentration and at considerably lower dosages. Both having the peptide predominantly as the monomer and treating with lower dosages dramatically reduce the cost of the treatment. For the third generation sequences

substitutions were made based on increasing conductance and anion selectivity. In an attempt to enhance anion selectivity by reintroducing a charged residue at or near the C-terminus of the W-substituted sequence, a series of doubly substituted peptides were prepared. Restoration of a positive charge near the C-terminus of the 22-residue peptide was first tested with regard to increasing throughput rates. A helical wheel projection of the M2GlyR-p22 helix revealed an even distribution of the polar residues. Not knowing where to optimally substitute an R, a series of M2GlyR peptides was prepared with R replacing one amino acid in each of the four C-terminal sequence positions.

NK_4-M2GlyR-p22 displayed concentration-response relationships similar to those observed with the 27 residue full-length CK_4-M2GlyR and NK_4-M2GlyR peptides. **Table 3** presents the summarized ion transport kinetic constants associated with the fitted lines presented in **Fig. 16**. NK_4-M2GlyR-p22 displayed a concentration-dependent response similar to that observed with the 27 residue full-length CK_4-M2GlyR and NK_4-M2GlyR peptides. NK_4-M2GlyR-p22 provided benchmark values for I_{MAX} of 23.7 ± 5.6 μAcm^{-2}, $k_{1/2}$ of 210 ± 70 μM, and Hill coefficient of 1.9 ± 0.6.

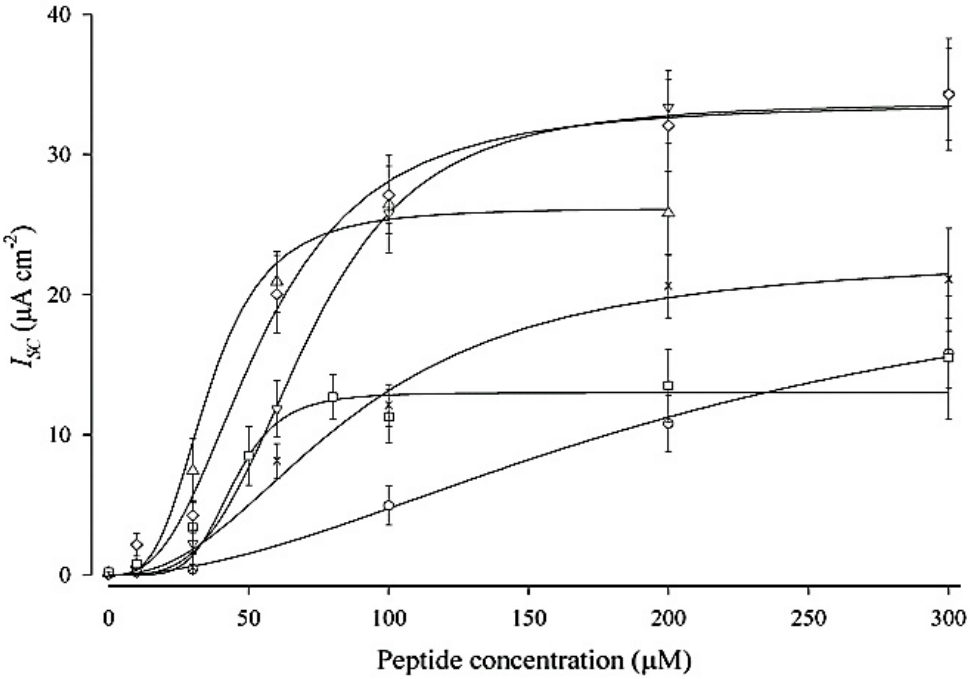

Fig. 16. Concentration-dependence of I_{SC} induced by NK_4-M2GlyR-p22 derived peptides with W and R amino acid substitutions on MDCK epithelial monolayers. Symbols represent the mean and standard error of 6 or greater observations for each concentration tested. Solid lines represent the best fit of a modified Hill equation to each data set. The NK_4-M2GlyR derived peptides concentration dependent I_{SC} curves are as follows: NK_4-M2GlyR-p22 (○), NK_4-M2GlyR-p22 S22W (□), NK_4-M2GlyR-p22 Q21R,S22W(Δ), NK_4-M2GlyR-p22 T20R,S22W(×), NK_4-M2GlyR-p22 T19R, S22W (▽) and NK_4-M2GlyR-p22 Q21W, S22R(◊).

Sequence	Replace-ment	Mr (Da)	Sol.(mM)	n	I_{MAX} (μA/cm²)	$k_{1/2}$ (μM)
KKKKPARVGLGITTVLTMTTQS	none	2358.9	11.1	1.9 ± 0.6	23.7 ± 5.6	210 ± 70
KKKKPARVGLGITTVLTMTTQW	S22W	2458.0	1.9	5.4 ± 2.9	13.0 ± 1.0	45
KKKKPARVGLGITTVLTMTTRW	Q21R, S22W	2486.1	4.9	3.3 ± 1.6	26.5 ± 3.2	36 ± 5
KKKKPARVGLGITTVLTMTRQW	T20R, S22W	2513.1	5.2	2.3 ± 0.8	22.7 ± 2.7	87 ± 15

Table 3. Characterization of M2GlyR derived peptides with W and R substitutions.

Introduction of a W in the presence and absence of the added R had a dramatic effect on the concentration required for half-maximal ion transport activity. The left-shifted $k_{1/2}$ values ranged from 36 to 87 μM as compared with the 210 μM observed for NK_4-M2GlyR-p22. Three of the doubly substituted sequences exhibited similar left shifts in the $k_{1/2}$ for anion transport when compared to NK_4-M2GlyR-p22 S22W. NK_4-M2GlyR-p22 T20R, S22W did not show this dramatic left-shift. The simplest interpretation is that the sequences with left-shifted $k_{1/2}$ values form homo-oligomeric supramolecular assemblies at lower concentrations than the benchmark peptide.

With regard to I_{MAX}, the doubly substituted sequences exhibited greater maximal transport rates relative to either NK_4-M2GlyR-p22 or C-terminal W substituted NK_4-M2GlyR-p22 S22W peptides. In the doubly substituted sequences the position of the R relative to the W also had an effect on I_{MAX}. The sequences which introduced R at positions 20 or 21, exhibited a greater I_{MAX} (22.7 ± 2.7 and 26.2 ± 3.2 μAcm^{-2}, respectively) than was observed with the W alone substituted sequence. These I_{MAX} values are similar to that seen for M2GlyR-p22. Introduction of the R at position 19 and inverting the R - W pair of sequence NK_4-M2GlyR-p22 Q21R, S22W to W - R resulted in even larger I_{MAX} values of 33.7 ± 1.3 and 33.6 ± 2.2 μAcm^{-2}, respectively. Most importantly, R substituted sequences showed greatly enhanced efficacy with I_{SC} values equaling I_{MAX} for M2GlyR-p22 with concentrations at or below 50 μM. The sum effect of changes in the kinetic parameters (I_{MAX} and $k_{1/2}$) is a substantial reduction in the peptide concentration required to attain ion transport rates that will likely be relevant in future basic and applied applications. With the exception of NK_4-M2GlyR-p22 T20R, S22W all of the other W and R containing sequences have greater Hill coefficients (3.3 ± 1.6 to 5.4 ± 2.9) than that calculated for NK_4-M2GlyR-p22 (2.1 ± 0.8). M2GlyR-p22 T20R, S22W had a Hill coefficient (2.8 ± 0.8) similar to that seen with NK_4-M2GlyR-p22. The increase in the Hill coefficients to values approaching five suggests that association/dissociation mechanisms in the bilayer are sensitive to structural changes in the peptide and consistent with the prediction that the channel pore is a homo-oligomeric supramolecular assembly that assembles by a complex or multistep mechanism.

As assessed in the Ussing chamber experiments, reintroduction of an R near the C-terminus in conjunction with the added W contributes another factor that influences the minimum concentrations required for assembly of a functional channel. Introduction of an R at, at any of the tested positions slightly decreases the Hill coefficient, suggesting that there is an energetic cost in forcing the R (transiently) across the acyl core of the phospholipids. Placing R either at position 19 or just outside the membrane appears to be optimal with regard to I_{MAX}, while an R placed at position 21 appears to be optimal with regard to $k_{1/2}$. Placing R at position 20 seems to be the least optimal position since the Hill coefficient, $k_{1/2}$ and I_{MAX}

show the lowest values within this peptide series. Computer modeling studies indicated that the R in any of the internal C-terminal positions could snorkel back toward the membrane to form a second membrane anchor. There is no evidence that the R in any of these substituted peptides is positioned with the side chain pointed into the water-filled lumen of the assembled pore.

In a parallel set of experiments designed to assess the role of the indole group in altering n, I_{MAX} and $k_{1/2}$ values (Derived from **Fig. 17** and summarized in **Table 4**), sequences were prepared that replaced the W with either F or Y. The F or Y substituted sequences, which also contain a second R substitution, exhibited greater solubility compared to their W-containing counterparts, with the exception of NK_4-M2GlyR-p22 Q21F, S22R. All of the aromatic amino acid containing sequences had lesser amounts of higher molecular weight associations in aqueous environments compared to the aromatic-free sequence. Predominantly monomer, with some dimer, is present in the cross-linked aromatic sequences.

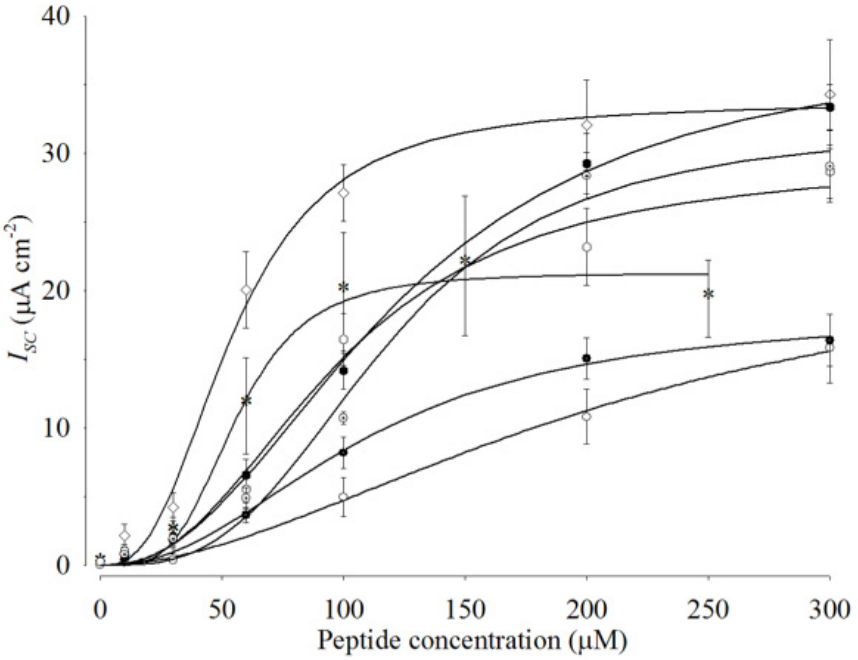

Fig. 17. Concentration-dependence of I_{SC} induced by NK_4-M2GlyR-p22 derived peptides with either F or Y and W amino acid substitutions on MDCK epithelial monolayers. Symbols represent the mean and standard error of 4 or greater observations for each concentration tested. Solid lines represent the best fit of a modified Hill equation to each data set. The NK_4-M2GlyR derived peptides dose dependent I_{SC} curves are as follows: NK_4-M2GlyR-p22 (○), NK_4-M2GlyR-p22 Q21W, S22R (◊), NK_4-M2GlyR-p22 Q21R, S22F (*), NK_4-M2GlyR-p22 T19R, S22F (closed hexagon), NK_4-M2GlyR-p22 Q21F, S22R (⊕), NK_4-M2GlyR-p22 Q21R, S22Y (open hexagon) and NK_4-M2GlyR-p22 T19R, S22Y (●).

Sequence	Replace-ment	Mr (Da)	Sol.(mM)	n	I_{MAX} (μA/cm²)	$k_{1/2}$ (μM)
KKKKPARVGLGITTVLTMTTRF	Q21R, S22F	2447.1	6.1	3.8 ± 2.5	21.3 ± 2.5	56 ± 8
KKKKPARVGLGITTVLTMRTQF	T19R, S22F	2474.1	12.2	2.3 ± 0.3	38.0 ± 2.3	120 ± 14
KKKKPARVGLGITTVLTMTTFR	Q21F, S22R	2447.1	21.0	3.1 ± 0.6	31.8 ± 3.6	120 ± 10

Table 4. Characterization of M2GlyR derived peptides with F/Y and R Substitutions.

The secondary structures of these peptides were measured in SDS micelles. CD spectra contained minima at 208 and 222 nm, similar to those seen for all other sequences, which indicate predominantly helical structures. Considering the lack of solution aggregation and similar CD profiles, we concluded that these sequences formed a similar hydrophobic fold (in solution) that prevents association or aggregation in aqueous solution, similar to that described above for other structures. In addition to stabilizing the concentration of monomer in aqueous solutions, inclusion of any C-terminal aromatic residue provided a lipid/water interfacial anchor. As was seen with W, F residues are commonly present (and Y to a lesser extent) at the hydrophobic/hydrophilic interface for TM segments of membrane proteins (Braun and von Heijne, 1999; Mall et al., 2000; Demmers et al., 2001; de Planque et al., 2003; Granseth et al., 2005; van der Wel et al., 2007; Hong et al., 2007). The data for sequences NK_4-M2GlyR-p22 and NK_4-M2GlyR-p22 Q21W, S22R are included as reference values. Comparing the F substituted sequences to those containing the paired W, the F-containing peptides displayed similar I_{MAX} but have right-shifted $k_{1/2}$ values. The Y variants gave mixed results relative to their W counterparts. NK_4-M2GlyR-p22 Q21R, S22Y showed a higher I_{MAX}, but had a right-shifted $k_{1/2}$ value while sequence NK_4-M2GlyR-p22 T19R, S22Y was inferior in both respects. With the exception of NK_4-M2GlyR-p22 Q21R, S22F, the $k_{1/2}$ values for the Y and F containing peptides are right-shifted relative to the W-containing peptides but left-shifted relative to the unmodified M2GlyR-p22.

Comparing all of the summarized data in **Tables 3 and 4** and the profiles shown in **Figs. 16 and 17**, the sequences displaying the highest ion transport activity and the second and third most left-shifted $k_{1/2}$ values are both W containing peptide sequences, NK_4-M2GlyR-p22 T19R, S22W and NK_4-M2GlyR-p22 Q21W, S22R. Based on the concentrations required for $k_{1/2}$, a rank ordering of the assembly-promoting effects of the C-terminal aromatic substitutions are as follows W > F >>Y. Given that when the R is placed at the C-terminus in NK4-M2GlyR-p22 Q21W, S22R will most likely cause further thinning of the membrane upon insertion (see **Fig. 17**), the sequence NK_4-M2GlyR-p22 T19R, S22W was chosen as a lead sequence for further analysis and modification.

Before committing to *in vivo* animal studies and preclinical trials, a few questions had to be addressed—did the lysine adduction and amino acid substitutions at T19R and S22W of the peptide alter its selectivity as an anion channel and did these modifications generate a potentially immunogenic structure?

NK_4-M2GlyR-p22 T19R, S22W was administered at clinically relevant dosages to the nasal passages of specific-pathogen-free female C57/BL6 mice to test for the induction of an immune response with or without cholera toxin (CT) a strong mucosal adjuvant. Lipopolycaccharide (LPS)-free peptide, when administered alone, induced very little peptide-specific immunity based on analyses of peptide-specific antibodies by enzyme-linked immunosorbent and enzyme-linked immunospot assays, induction of cytokine production, and delayed-type hypersensitivity (DTH) responses. The administration of NK_4-M2GlyR-p22 T19R, S22W with CT induced peptide-specific immunoglobulin G (IgG) antibodies, DTH responses and a Th2-dominant cytokine response. Co-administration of CT induced a systemic NK_4-M2GlyR-p22 T19R, S22W-specific IgG response but not a mucosal peptide-specific antibody response. The lack of peptide-specific immunity and specifically mucosal immunity should allow repeated NK_4-M2GlyR-p22 T19R, S22W peptide applications to epithelial surfaces to correct ion channelopathies (van Ginkel et al., 2008).

Results indicate that additional modifications are necessary to achieve the desired anion selectivity. NK_4-M2GlyR-p22 T19R, S22W was tested in artificial bilayers composed of **1-palmitoyl-2-oleoyl-sn-glycero-3-phosphocholine:1-palmitoyl-2-oleoyl-sn-glycero-3-phospho-L-serine (**POPC:POPS, 70:30) and in *Xenopus* oocytes. In both cases the selectivity for monovalent anions relative to monovalent cations had dropped to a value slightly above unity, indicating that the pore formed was only slightly anion selective. Computer simulations were employed as an initial strategy to determine the most promising structures for synthesis and testing. Before those simulations could be conducted, the identity of the pore-forming residues had to be established. The structure of NK_4-M2GlyR-p22 T19R, S22W was analyzed by solution NMR as a monomer in detergent micelles and simulated as five-helix bundles in a membrane environment. Details of helix packing and residue distribution of the pore were analyzed. Results summarized in **Fig. 18a** demonstrate that the pore is mainly lined with A6, R7, L10, T13, T14, T17, T20 and Q21. Note the N- and C-terminal residues, K1-4 and W22, should not be considered as pore lining, even though they are indicated to have high pore-lining probabilities based on their contacts with (bulk) water molecules. The predicted pore-lining interface is largely consistent with the one derived from consideration of amphipathicity. However, the predicted pore-lining interface is broader due to substantial fluctuations of the pore. Participation of residues in helix-helix packing is characterized by calculating the average burial areas of side-chains, shown in **Fig. 18b**. Clearly, most residues with the structured region contribute to helix-helix interactions, except G9, G11, I12, V15 and R19. These residues either lack side chains (G9 and G11) or are fully membrane exposed. (I12, V15, L16 and R19). L10 and Q21 appear to be particularly important for stabilization of the pore assembly with the largest buried surface areas. Ongoing studies are guided by the hypothesis that alterations in one or more of the following parameters-- hydrogen bonding potentials of pore lining residues, electrostatics of pore lining residues, pore length or pore rigidity--will affect anion selectivity. By defining which of these elements increase selectivity we will elucidate how selectivity filters and permeation rates might be modulated so that an optimal sequence to allow for highly-selective Cl^- permeation can be developed. Current experiments are designed to examine the effect of adding the positively charged amino acid L-diaminopropionic acid (DAP; R= CH_2-$^+NH_3$). Computer Modeling studies were performed on both singly and doubly DAP-substituted sequences (**Fig. 19**). Modeling the Potential of Mean Force (PMF) for moving different ions from one side of the channel to the other predicted similar permeabilities through NK_4-M2GlyR-p22 T19R, S22W for both Cl^- and Na^+, while

introduction of the cationic DAP residues favored the passage of Cl^-. The double-substituted T13Dap, T20Dap sequence shows the smallest energy wells where Cl^- could become trapped, suggesting that it could be a preferred sequence.

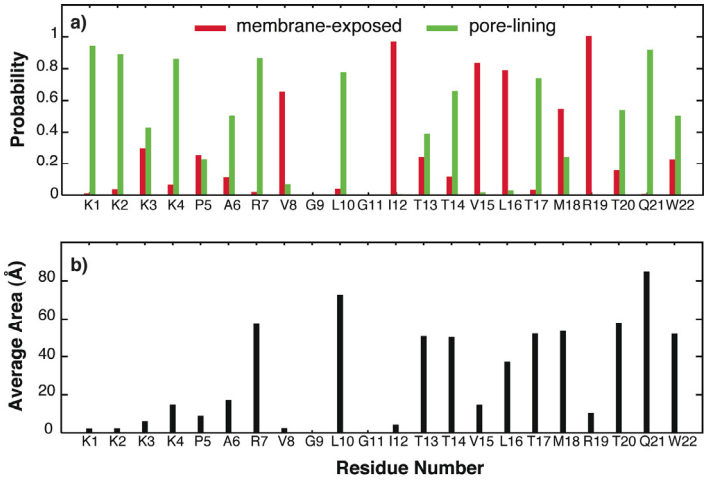

Fig. 18. **a.** Probabilities of a residue being either a pore-lining one or a membrane-exposed one. **b.** Average surface area of burial due to peptide-peptide interactions. The results are calculated from the last 80 ns of 100 ns production simulation of the left-handed channel.

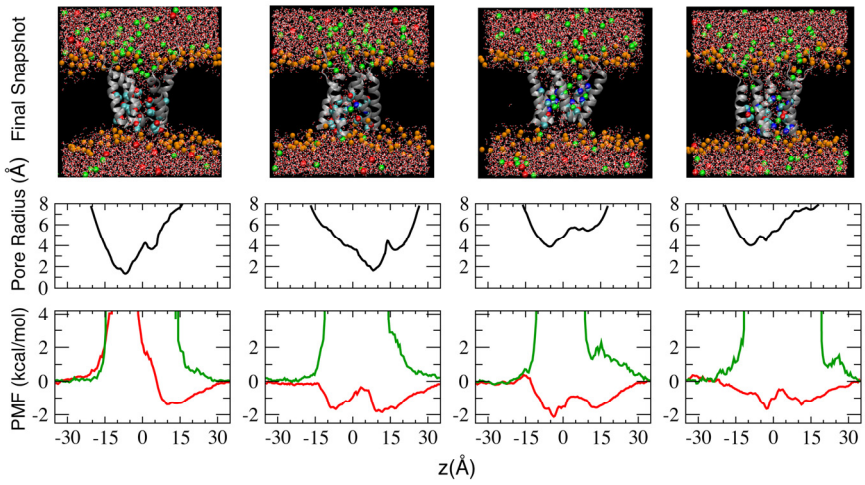

Fig. 19. Summary of the preliminary simulations of NK_4-M2GlyR-p22 T19R, S22W (lane 1) and its several singly (lane 2, T17Dap) and doubly Dap substituted sequences (lane 3, T13Dap,T17Dap; lane 4, T13Dap,T20Dap). The lengths of the simulations are at least 20 ns. The pore profiles were computed using the HOLE program based on the last snapshots shown. The PMFs were computed from equilibrium ion densities. The red line signifies chloride and the green line sodium.

Surprisingly, in generating more cationic channel-forming sequences, assembly, as assessed *in silico*, was not hampered by the presence of inter-peptide charge repulsion between the amino groups on adjacent helical segments. This repulsion appears to be accommodated by a widening of the pore. It might also cause the helices to adopt a staggered registry; however, these modeling studies have not indicated that outcome. Computer modeling of the M2GlyR-p22 T19R, S22W pore predicts the diameter to be about 4-5 Å at the narrowest portion of the channel (position T17). As stated above, modeling indicates that widening of the pore by the introduction of cationic residues results in a shift of the narrowest part of the pore to L10 with about the same pore diameter. The sequences containing multiple DAP residues appear to increase the diameter of the pore to ~8 Å, potentially leading to the passage of larger anions that were previously impermeable (glutamate, isethionate, etc.) and/or increased conductance. Preliminary results indicate that all of the DAP substituted sequences generate ion fluxes both across MDCK monolayers and in *Xenopus* oocytes. Permselectivity, however, remains to be determined.

NK_4-M2GlyR p-22 peptides with both W and R substitutions near the C terminus appear to be optimal structures for ongoing development of a therapeutic agent. These structures exhibited the greatest net ion flux and were among the most potent of the peptides assessed. Importantly, a mucosal immune response was not observed following exposure to these structures. The greatest challenge for ongoing development is the establishment of high anion to cation selectivity. Pore and lipid interfacial side chains have been identified to provide key information that is being used to build new structures in silico. These new structures are now being tested for ion throughput and selectivity. In addition to developing a potentially therapeutic structure, the outcomes of these experiments will provide a wealth of information regarding the contributions of hydrogen bonding, electrostatics, and pore rigidity to ion selectivity.

5. Summary

Nearly seventy-five years have passed since cystic fibrosis of the pancreas was first described as a unique clinical syndrome that was associated with failure to thrive and death in early childhood. The underlying cause of the disease, the absence of an epithelial anion conductance, was determined in the early 1980s and the gene coding for this anion channel was identified by the end of that decade. Even though the underlying cause has been known for more than twenty years, a curative treatment has not been developed, even at the tissue or organ level. Through the years, numerous therapies have been implemented – some with more positive outcomes than others. The commonality of all therapies is their palliative nature – there is no cure for CF although there are promising therapies in the pipeline for some subsets of the patient population (e.g., VX-770 for patients harboring G551D mutations). Supplemental pancreatic enzymes, more potent antibiotics and targeted delivery systems, daily respiratory therapy and the use of anti-inflammatory agents have added years to the typical lifespan and have greatly enhanced the quality of life of those suffering from CF. Nonetheless, additional therapeutic options are needed to address both tissue-specific and generalized disease progression. A synthetic anion-selective channel that can be delivered directly to epithelial cell membranes will provide one such option for improved health.

This line of investigation has as its primary goal to create a therapeutic channel-forming peptide that can be delivered from aqueous solution, insert itself into cell membranes and

provide a pathway that is selective for the permeation of anions. The synthetic peptide should be effective at low aqueous concentrations, persistent in the membrane, and should not be antigenic. A particular benefit of this approach is that the therapy could be effective independent of the genetic mutation(s) expressed by each patient.

The development of synthetic channel-forming peptides has progressed through a series of stages including discovery, initial implementation or proof of concept, and optimization for various physical, biochemical and physiological endpoints. The glycine receptor, a naturally occurring anion selective channel, was selected as the simplest chassis from which to start the process. The M2 segment, which constitutes the pore of the pentameric receptor, was used to demonstrate that exogenously applied peptides could support anion movement across an epithelium. This peptide was modified with the addition of lysine residues to increase aqueous solubility and a truncated version was found to be equally effective, which reduced a portion of the burden of peptide synthesis. The truncated version was further modified to establish an anchor at the membrane:water interface. Together, these modifications yielded a peptide that is effective at aqueous concentrations below 50 micromolar and that persists in the epithelium for hours. At various stages in this project, results have shown that the peptides have the desired effects on electrophysiology when tested in murine nasal epithelia and the peptides appear not to induce a mucosal immune response, even when administered with cholera toxin as an adjuvant. Although the underlying mechanism remains to be determined, channel forming peptides were also associated with an increase in glutathione release from CF cells, which also constitutes a therapeutic outcome. Overall, the line of investigation has yielded much new knowledge regarding the design and construction of ion channels. Ongoing studies are focused to modify the ion selectivity of the channel, i.e., to build an anion selective channel for therapeutics and to determine the contribution of structural elements to channel ion selectivity. Clearly, there continues to be a need for new and novel therapies to treat the many aspects of CF. Synthetic anion selective channels constitute a therapeutic modality that has great potential to improve the lives of these patients.

6. Acknowledgements

We thank Gary Radke, Takeo Iwamoto Ph.D., Robert Brandt and Ryan Carlin for their technical assistance. We thank Professor Jianhan Chen for his assistance in redrawing computer simulation figures. This article is contribution no. 12-054-B from the Kansas Agricultural Experiment Station. Manhattan, KS-66506. This study has been supported in part by United States of America PHS grants form the National Institutes of Health to JMT: DK61866, GM43617 and GM074096.

7. References

Accurso, F.J., Rowe, S.M., Clancy, J.P., Boyle, M.P., Dunitz, J.M., Durie, P.R., Sagel, S.D., Hornick, D.B., Konstan, M.W., Donaldson, S.H., Moss, R.B., Pilewski, J.M., Rubenstein, R.C., Uluer, A.Z., Aitken, M.L., Freedman, S.D., Rose, L.M., Mayer-Hamblett, N., Dong, Q., Zha, J., Stone, A.J., Olson, E.R., Ordoñez, C.L., Campbell, P.W., Ashlock, M.A., Ramsey, B.W. (2010) Effect of VX-770 in persons with cystic fibrosis and the G551D-CFTR mutation. *N Engl J Med*. 363(21):1991-2003.

Alexander, C., Ivetac, A., Liu, X., Norimatsu, Y., Serrano, J.R., Landstrom, A., Sansom, M., Dawson, D.C. (2009) Cystic fibrosis transmembrane conductance regulator: using differential reactivity toward channel-permeant and channel-impermeant thiol-reactive probes to test a molecular model for the pore. *Biochemistry*. 2048(42):10078-10088.

Atkuri, K.R., Mantovani, J.J., Herzenberg, L.A., Herzenberg, L.A. (2007) N-Acetylcysteine-a safe antidote for cysteine/glutathione deficiency. *Current Opinion in Pharmacology* 7:355-359.

Baer, M., Sawa, T., Flynn, P., Luehrsen, K., Martinez, D., Wiener-Kronish, J.P., Yarranton, G., Bebbington, C. (2009) An engineered human antibody Fab fragment specific for Pseudomonas aeruginosa PcrV antigen has potent anti-bacterial activity. *Infect Immun*. 77(3):1083-1090.

Beck, E.J., Yang, Y., Yaemsiri, S., Raghuram, V. (2008) Conformational changes in a pore-lining helix coupled to cystic fibrosis transmembrane conductance regulator channel gating. *J Biol Chem*. 283:4957-4966.

Bilton, D., Robinson, P., Cooper, P., Gallagher, C., Kolbe, J., Fox, H., Jaques, A., Charlton, B. (2011) Inhaled dry powder mannitol in cystic fibrosis: An efficacy and safety study. *Eur Respiratory J*. 38(5):1071-1080.

Brady, K.G., Kelley, T.J., Drumm, M.L. (2001) Examining basal chloride transport using the nasal potential. *Am J Physiol Lung Cell Mol Physiol*. 281(5):L1173-1179.

Braun, P., von Heijne, G. (1999) The aromatic residues Trp and Phe have different effects on the positioning of a transmembrane helix in the microsomal membrane. *Biochemistry* 38:9778-9782.

Broughman, J.R., Shank, L.P., Iwamoto, T., Prakash, O., Schultz, B.D., Tomich, J.M., Mitchell, K.E. (2002) Structural implications of placing cationic residues at either the NH2- or COOH- terminus in a pore-forming synthetic peptide. *J Membrane Biol*. 190:93-103.

Broughman, J.R., Shank, L.P., Takeguchi, W., Iwamoto, T., Mitchell, K.E., Schultz, B.D., Tomich, J.M. (2002) Distinct structural elements that direct solution aggregation and membrane assembly in the channel-forming peptide M2GlyR. *Biochemistry* 41:7350-7358.

Broughman, J.R., K. Mitchell, T. Iwamoto, B.D. Schultz, J.M. Tomich. (2001) Amino-terminal modification of a channel forming peptide increases capacity for epithelial anion secretion. *Am. J. Physiol: (Cell Physiol.)* 280:C451-458.

Cheer, S.M., Waugh, J., Noble, S. (2003) Inhaled tobramycin (TOBI): a review of its use in the management of *Pseudomonas aeruginosa* infections in patients with cystic fibrosis. *Drugs* 63:2501-2520.

Chen, X., Kube, D.M., Cooper, M.J., Davis, P.M. (2007) Cell Surface Nucleolin Serves as Receptor for DNA Nanoparticles Composed of Pegylated Polylysine and DNA. *Molecular Therapy* 16:333–342.

Cook, G.A., Prakash, O., Zhang, K., Shank, L.P., Takeguchi, W.A., Robbins, A., Gong, Y.X., Iwamoto, T., Schultz, B.D., Tomich, J.M.. (2004) Activity and structural comparisons of solution associating and monomeric channel-forming peptides derived from the glycine receptor M2 segment. *Biophys J*. 86(3):1424-1435.

Corry, B., Chung, S.H. (2006) Mechanisms of valence selectivity in biological ion channels. *Cell Mol Life Sci*. 63:301-315.

Dawson, D.C., Smith, S.S., Mansoura, M.K. (1999) CFTR: Mechanism of anion conduction. *Physiol Rev*. 79(1 Suppl):S47-75.

de Planque, M.R., Bonev, B.B., Demmers, J.A., Greathouse, D.V., Koeppe, R.E. 2nd, Separovic, F., Watts, A. and Killian, J.A. (2003) Interfacial anchor properties of tryptophan residues in transmembrane peptides can dominate over hydrophobic matching effects in peptide-lipid interactions. *Biochemistry* 42:5341-5348.

Demmers, J.A., van Duijn, E., Haverkamp, J., Greathouse, D.V., Koeppe, R.E. 2nd, Heck, A.J., Killian, J.A. (2001) Interfacial positioning and stability of transmembrane peptides in lipid bilayers studied by combining hydrogen/deuterium exchange and mass spectrometry. *J Biol. Chem*. 276:34501-34508.

Donaldson, S.H., Bennett, W.D., Zeman, K.L., Knowles, M.R., Tarran, R., Boucher, R.C. (2006) Mucus Clearance and Lung Function in Cystic Fibrosis with Hypertonic Saline. *New England Journal of Medicine* 354(3):1848-1851.

Dormer, R.L., Harris, C.M., Clark, Z., Pereira, M.M.C., Doull, I.J.M., Norez, C., Becq F., McPherson, M.A. (2005) Sildenafil (Viagra) corrects ΔF508-CFTR location in nasal epithelial cells from patients with cystic fibrosis. *Thorax* 60:55–59.

Dutzler, R., Campbell, E.B., Cadene, M., Chait, B.T., MacKinnon, R. (2002) X-ray structure of a ClC Cl- channel at 3.0 A reveals the molecular basis of anion selectivity. *Nature* 415(6869):287-294.

Dutzler, R., Campbell, E.B., MacKinnon, R. (2003) Gating the selectivity filter in ClC Cl- channels. *Science* 300:108-112.

Dutzler, R., E.B. Cambell, M. Cadene, B.T. Chait, and R. MacKinnon. (2002) X-ray structure of a ClC chloride channel at 3.0 Å reveals the molecular basis of anion selectivity. *Nature* 415:287-294.

Elkins, M.R., Robinson, M., Rose, B.R., Harbour, C., Moriarty, C.P., Marks, G.B., Belousova, E.G., Xuan, W., Bye, P.T. (2006) A controlled trial of long-term inhaled hypertonic saline in patients with cystic fibrosis. *N Engl J Med*. 354:229-240.

Estévez, R., Jentsch, T. (2002) CLC chloride channels: correlating structure with function. *Current Opinion in Structural Biology* 12:531-539.

Fuchs, H.J., Borowitz, D.S., Christiansen, D.H., Morris, E.M., Nash, M.L., Ramsey, B.W., Rosenstein, B.J., Smith, A.L., Wohl, M.E. (1994) Effect of aerosolized recombinant human DNase on exacerbations of respiratory symptoms and on pulmonary function in patients with cystic fibrosis. *N Engl J Med* 331:637-642.

Freedman, S.D., Katz, M.H., Parker, E.M., Laposata, M., Urman, M.Y., Alvarez, J.G. (1999) A membrane lipid imbalance plays a role in the phenotypic expression of cystic fibrosis in cftr (-/-) mice. *Proc. Natl. Acad. Sci. USA* 96:13995-14000.

Freedman, S.D., Blanco, P.G., Zaman, M.M., Shea, J.C., Ollero, M., Hopper, I.K., Weed, D.A., Gelrud, A., Regan, M.M., Laposata, M., Alvarez, J.G., O'Sullivan, B.P. (2004) Association of cystic fibrosis with abnormalities in fatty acid metabolism. *N Engl J Med*. 350:560-569.

Gao, L., Kim, K.J., Yankaskas, J.R., and Forman, H.J. (1999) Abnormal glutathione transport in cystic fibrosis airway epithelia. *Am J Physiol Lung Cell Mol Physiol* 277:L113–L118.

Gao, L., Broughman, J.R., Iwamoto, T., Tomich, J.M., Venglarik, C.J., Forman, H.J. (2001) Synthetic Cl- channel restores glutathione secretion in airway epithelia. *Am. J. Physiol. (Lung)* 281: L24-L30.

Gibson, R.L., Burns, J.L., Ramsey, B.W. (2003) Pathophysiology and management of pulmonary infections in cystic fibrosis. *Am J Respir Crit Care Med*. 168:918–951.

Granseth, E., von Heijne, G., Elofsson, A. (2005) A study of the membrane-water interface region of membrane proteins. *J Mol. Biol*. 346(1):377-385.

Grasemann, H., Stehling, F., Brunar, H., Widmann, R., Laliberte, T.W., Molina, L., Doring, G., Ratjen, F. (2007) Inhalation of Moli1901 in patients with cystic fibrosis. *Chest* 131:1461–1466.

Gunthorpe, M.J., Lummis, S.C. (2001) Conversion of the ion selectivity of the 5-HT(3a) receptor from cationic to anionic reveals a conserved feature of the ligand-gated ion channel superfamily. *J Biol Chem*. 276:10977-10983.

Harzer, U., Bechinger, B. (2000) Alignment of lysine-anchored membrane peptides under conditions of hydrophobic mismatch: a CD, ^{15}N and ^{31}P solid-state NMR spectroscopy investigation. *Biochemistry* 39:13106-13114.

Herrera, A.I., Al-Rawi, A., Cook G.A., Prakash, O., Tomich, J.M., Chen, J. (2010) Introduction of a C-Terminal Tryptophan in a Pore-Forming Peptide: A Structure/Activity Study. *PROTEINS: Structure, Function, and Genetics* 78(10): 2238-2250.

Hilf, R.J., Dutzler, R. (2008) X-ray structure of a prokaryotic pentameric ligand-gated ion channel. *Nature* 452:375-380.

Hong, H., Park, S., Jiménez, R.H., Rinehart, D., Tamm, L.K. (2007) Role of aromatic side chains in the folding and thermodynamic stability of integral membrane proteins. *J. Am. Chem. Soc.* 129(26):8320-8327.

Ivanov, I., Cheng, X., Sine, S.M., McCammon, J.A. (2007) Barriers to ion translocation in cationic and anionic receptors from the Cys-loop family. *J Am Chem Soc*. 129:8217-8224.

Iwamoto, T., Grove, A., Montal, M. O., Montal, M., Tomich, J. M. (1994) Chemical synthesis and characterization of peptides and oligomeric proteins designed to form transmembrane ion channels. *Int. J. Peptide Protein Res*. 43:597-607.

Jaques, A., Daviskas, E., Turton, J.A., McKay, K., Cooper, P., Stirling, R.G., Robertson, C.F., Bye, P.T., Lesouëf, P.N., Shadbolt, B., Anderson, S.D., Charlton, B. (2008) Inhaled mannitol improves lung function in cystic fibrosis.Chest 133(6):1388–1396.

Jayasinghe, S., Hristova, K., White S.H.(2001) Energetics, stability, and prediction of transmembrane helices. *J Mol Biol*. 312:927-934.

Jensen, M.L., Pedersen, L.N., Timmermann, D.B., Schousboe, A., Ahring, P.K. (2005) Mutational studies using a cation-conducting GABA-A receptor reveal the selectivity determinants of the Cys-loop family of ligand-gated ion channels. *J Neurochem*. 92:962-972.

Jensen, M.L., Schousboe, A., Ahring, P.K. (2005) Charge selectivity of the Cys-loop family of ligand-gated ion channels. *J Neurochem*. 92:217-225.

Kellerman, D., Mospan, R., Engels, J., Schaberg, A., Gorden, J., Smiley, L. (2008) Denufosol: A review of studies with inhaled P2Y(2) agonists that led to phase 3. *Pulm Pharmacol Ther*. 21:600–607.

Keramidasa, A., Moorhousea, A.A., Schofieldb, P.R. and Barry, P.H. (1994) Ligand-gated ion channels: mechanisms underlying ion selectivity. *Progress in Biophysics & Molecular Biology* 86:161–204.

Konstan, M.W., Byard, P.J., Hoppel, C.L., Davis, P.B. (1995) Effect of high-dose ibuprofen in patients with cystic fibrosis. *N Engl J Med*. 332:848–854.

Konstan, M.W., Davis, P.B., Wagener, J.S., Hilliard, K.A., Stern, R.C., Milgram, L.J.H., Kowalczyk, T.H., Hyatt, S.L., Fink, T.L., Gedeon, C.R., Oette, S.M., Payne, J.M., Muhammad, O., Ziady, A.G., Moen, R.C., Cooper, M.J. (2004)Compacted DNA nanoparticles administered to the nasal mucosa of cystic fibrosis subjects are safe and demonstrate partial to complete cystic fibrosis transmembrane regulator reconstitution. *Hum Gene Ther*. 15:1255–1269.

Lazaar, A.L., Sweeney, L.E., MacDonald, A.J., Alexis, N.E., Chen, C., Tal-Singer, R. (2011) SB-656933, a novel CXCR2 selective antagonist, inhibits ex-vivo neutrophil activation and ozone-induced airway inflammation in humans. *British Journal of Clinical Pharmacology*. 72(2):282-293.

Linsdell, P. (2006) Mechanism of chloride permeation in the cystic fibrosis transmembrane conductance regulator chloride channel. *Exp Physiol*. 91:123-129.

Liu, X., Smith, S.S., Sun, F., Dawson, D.C. (2001) CFTR: Covalent modification of cysteine-substituted channels expressed in Xenopus oocytes shows that activation is due to the opening of channels resident in the plasma membrane. *J Gen Physiol*. 118:433-46.

Lobet, S., Dutzler, R. (2006) Ion-binding properties of the ClC chloride selectivity filter. *EMBO J*. 25:24-33.

Lowry, F. (2011) FDA Panel Sends Liprotamase Back to the Drawing Board. Medscape Medical News. http://www.medscape.com/viewarticle/735722

Mall, S., Broadbridge, R., Sharma, R.P., Lee, A.G., East J.M. (2000) Effects of aromatic residues at the ends of transmembrane alpha-helices on helix interactions with lipid bilayers. *Biochemistry* 39:2071-2078.

Mansoura, M.K., Smith, S.S., Choi, A.D., Richards, N.W., Strong, T.V., Drumm, M.L., Collins, F.S., Dawson, D.C. (1998) Cystic fibrosis transmembrane conductance regulator (CFTR) anion binding as a probe of the pore. *Biophys J*. 74:1320-1332.

Marsh, D. (1996) Peptide models for membrane channels. *Biochem J*. 315(Pt 2):345-361.

Mitaku, S., Hirokawa, T., Tsuji T. (2002) Amphiphilicity index of polar amino acids as an aid in the characterization of amino acid preference at membrane-water interfaces. *Bioinformatics* 18:608-616.

Miyazawa, A., Fujiyoshi, Y., Unwin, N. (2003) Structure and gating mechanism of the acetylcholine receptor pore. *Nature* 424:949-955.

Montal, M.O., Reddy, G.L., Iwamoto, T., Tomich, J.M., Montal, M. (1994) Identification of an ion channel-forming motif in the primary structure of CFTR, the Cystic Fibrosis Cl-channel. *Proc. Natl. Acad. Sci. USA* 91:1495-1499.

Mutter, M., Hersperger, R., Gubernator, K., Müller, K. (1989) The construction of new proteins: V. A template-assembled synthetic protein (TASP) containing both a 4-helix bundle and beta-barrel-like structure. *Proteins* 5(1):13-21.

Pettit, R.S. and Johnson, C.E. (2011) Airway-rehydrating agents for the treatment of cystic fibrosis: past, present, and future. *Ann. Pharmacother* 45:49-59.

Pollack, A. (2011) Vertex says trial of Vertex's VX-770, a cystic fibrosis drug, eased breathing - NYTimes.com. The Business of Health Care - Prescriptions Blog - NYTimes.com. http://prescriptions.blogs.nytimes.com/2011/02/23/vertex-says-cystic-fibrosis-drug-helped-patients-breathe-easier/

Ramalho, A.S., Beck, S., Meyer, M., Penque, D., Cutting, G.R., Amaral, M.D. (2002) Five percent of normal cystic fibrosis transmembrane conductance regulator mRNA ameliorates the severity of pulmonary disease in cystic fibrosis. *Am J Respir Cell Mol Biol.* 27:619–627.

Reddy, L.G., Iwamoto, T., Tomich, J.M. and Montal, M. (1993) Synthetic peptides and four-helix bundle proteins as model systems for the pore-forming structure of channel proteins. III. Transmembrane segment M2 of the brain glycine receptor channel is a plausible candidate for the pore-lining structure. *J. Biol. Chem*. 268:14608-14615.

Retsch-Bogart, G. (2011) Role of new therapies in CF lung disease. CF Learning Center
http://www.cflearningcenter. com /pdfs/CFLC2011/healthcare/Role_of_New_Therapies_in_CF_Lung_Disease.pdf

Riordan, J.R. (2008) CFTR Function and Prospects for Therapy. *Annu Rev Biochem*. 77:701-726

Saiman, L., Marshall, B.C., Mayer-Hamblett, N., Burns, J.L., Quittner, A.L., Cibene, D.A., Coquillette, S., Fieberg, A.Y., Accurso, F.J., Campbell, P.W. 3rd. (2003) Azithromycin in patients with cystic fibrosis chronically infected with Pseudomonas aeruginosa: a randomized controlled trial. *J A M A* 290:1749–1756.

Sagel, S.D., Sontag, M.K., Anthony, M.M., Emmett, P., Papas, K.A. (2011). Effect of an antioxidant-rich multivitamin supplement in cystic fibrosis. *J Cystic Fibrosis* 10(1):31-36.

Schmieden, V., Grenningloh, G., Schofield, P.R., Betz, H. (1989) Functional expression in Xenopus oocytes of the strychnine binding 48 kd subunit of the glycine receptor. *EMBO J*. 8:695-700.

Sears, H., Gartman, J., Casserly, P. (2011) Treatment options for cystic fibrosis: State of the art and future perspectives. *Reviews on Recent Clinical Trials* 6(2):94-107.

Shank, L.P., Broughman, J.R., Brandt, R.M., Robbins, A.S., Takeguchi, W., Cook, G.A., Hahn, L., Radke, G., Iwamoto, T., Schultz, B.D., Tomich, J.M. (2006) Redesigning channel-forming peptides: amino acid substitutions in channel- forming peptides that enhance rates of supramolecular assembly and raise ion transport activity. *Biophys J*. 90:2138-2150.

Sheridan, C. (2011) First cystic fibrosis drug advances towards approval. *Nature Biotechnology*, 29(6):465-466.

Sine, S.M., Engel, A.G. (2006) Recent advances in cys-loop receptor structure and function. *Nature* 440:448-455.

Smith, S.S., Liu, X., Zhang, Z.R., Sun, F., Kriewall, T.E., McCarty, N.A., Dawson, D.C. (2001) CFTR: Covalent and noncovalent modification suggests a role for fixed charges in anion conduction. *J Gen Physiol*. 118:407-431.

Sunesen, M., de Carvalho, L.P., Dufresne, V., Grailhe, R., Savatier-Duclert, N., Gibor, G., Peretz, A., Attali, B., Changeux, J.P., Paas, Y. (2006) Mechanism of Cl- selection by a glutamate-gated chloride (GluCl) receptor revealed through mutations in the selectivity filter. *J Biol Chem*. 281:14875-14881.

Tang, P., Mandal, P.K., Xu, Y. (2002) NMR structures of the second transmembrane domain of the human glycine receptor alpha(1) subunit: model of pore architecture and channel gating. *Biophys J*. 83:252-262.

Tirouvanziam, R., Conrad, C.K., Bottiglieri, T., Herzenberg, L.A., Moss, R.B. (2006) High-dose oral N-acetylcysteine, a glutathione prodrug, modulates inflammation in cystic fibrosis. *Proc Natl Acad Sci USA* 103:4628–4633.

Tomich, J.M., Wallace, D.P., Henderson, K., Brandt, R., Ambler, C.A., Scott, A.J., Mitchell, K.E., Radke, G., Grantham, J. J. Sullivan, L.P., Iwamoto, T. (1998) Aqueous solubilization of transmembrane peptide sequences with retention of membrane insertion and function. *Biophys J*. 74:256-267.

Unwin, N. (2003) Structure and action of the nicotinic acetylcholine receptor explored by electron microscopy. *FEBS Lett*. 555:91-95.

Unwin, N. (2005) Refined structure of the nicotinic acetylcholine receptor at 4Å resolution. *J Mol Biol*. 346:967-989.

van der Wel, P.C.A., Reed, N.D., Greathouse, D.V., Koeppe, R.E.II (2007) Orientation and motion of tryptophan interfacial anchors in membrane-spanning peptides *Biochemistry* 46(25):7514-7524.

Vogt, B., Ducarme, P., Schinzel, S., Brasseur, R., Bechinger, B. (2000) The topology of lysine-containing amphipathic peptides in bilayers by circular dichroism, solid-state NMR, and molecular modeling. *Biophys J.* 79:2644-2656.

Vogt, B., Ducarme, P., Schinzel, S., Brasseur, R., Bechinger, B. (2000) The topology of lysine-containing amphipathic peptides in bilayers by circular dichroism, solid-state NMR, and molecular modeling. *Biophys J.* 79:2644–2656.

Wallace, D.P., Tomich, J.M., Eppler, J., Iwamoto, T., Grantham, J.J., Sullivan, L.P. (2000) A Channel forming peptide induces Cl^- secretion by T84 cells: Modulation by Ca^{2+}-dependent K^+ channels. *Biochem Biophys Acta* 1464:69-82.

Wallace, D.P., Tomich, J.M., Iwamoto, T., Henderson, K., Grantham, J.J., Sullivan, L.P. (1997) A synthetic peptide derived from the glycine-gated Cl^- channel generates Cl^- and fluid secretion by epithelial monolayers. *Am J Physiol: (Cell Physiol)* 272:C1672-C1679.

Wilschanski, M., Miller, L., Shoseyov, D., Blau, H., Rivlin, J., Aviram, M., Cohen, M., Armoni, S., Yaakov, Y., Pugatch, T., Cohen-Cymberknoh, M., Miller, N.L., Reha, A., Northcutt, V.J., Hirawat, S., Donnelly, K., Elfring, G.L., Ajayi, T., Kerem, E. (2011) Chronic ataluren (PTC124) treatment of nonsense mutation cystic fibrosis. *Eur Respiratory J.* 38(1):59-69.

Wimley W.C., White, S.H. (1996) Experimentally determined hydrophobicity scale for proteins at membrane interfaces. *Nat Struct Biol.* 3:842-848.

Wimley, W.C., White, S.H. (1999) Membrane protein folding and stability: physical principles. *Ann Rev Biomol Struct.* 28:319-365.

Wimley, W.C., White, S.H. (2000) Designing Transmembrane α-Helices That Insert Spontaneously. *Biochemistry* 39:4432-4442.

Yankaskas, J.R., (1993) Papilloma virus immortalized tracheal epithelial cells retain a well-differentiated phenotype. *Am J Physiol Cell Physiol.* 264:C1219–C1230.

Yushmanov, V.E., Mandal, P.K., Liu, Z., Tang, P., Xu, Y. (2003) NMR structure and backbone dynamics of the extended second transmembrane domain of the human neuronal glycine receptor α_1 subunit. *Biochemistry* 42:3989-3995.

Zerhusen, B., Zhao, J., Xie, J., Davis, P.B., Ma, J. (1999) A single conductance pore for Cl- ions formed by two cystic fibrosis transmembrane conductance regulator molecules. *J Biol Chem.* 274:7627-7630.

Zhang, L., Aleksandrov, L.A., Riordan, J.R., Ford, R.C. (2011) Domain location within the cystic fibrosis transmembrane conductance regulator protein investigated by electron microscopy and gold labelling. *Biochim Biophys Acta*. 1808(1):399-404.

Zhang, Z.R., McDonough, S.I., McCarty, N.A. (2000) Interaction between permeation and gating in a putative pore domain mutant in the cystic fibrosis transmembrane conductance regulator. *Biophys J.* 79:298-313.

Zhang, X.D., Li, Y., Yu, W.P., Chen, T.Y. (2006) Roles of K149, G352, and H401 in the channel functions of ClC-0: testing the predictions from theoretical calculations. *J Gen Physiol*. 127:435-447.

Zhou, Z., Hu, S., Hwang, T.C. (2002) Probing an open CFTR pore with organic anion blockers. *J Gen Physiol*. 120:647-662.